Diverse Consequences in Liver Injury in Mice with Different Autophagy Functional Status Treated with Alcohol

Shengmin Yan[1], Jun Zhou[1, 2], Xiaoyun Chen[1], Zheng Dong [3, 4], Xiao-Ming Yin[1, 3]*

[1]Department of Pathology and Laboratory Medicine, Indiana University School of Medicine Indianapolis, IN 46202, USA

[2]Departments of Minimal Invasive Surgery, and [3]Nephrology, The Second Xiangya Hospital, Central South University, Changsha, China

[4]Department of Cell Biology and Anatomy, Medical College of Georgia and Charlie Norwood VA Medical Center, Augusta, GA

Short running title: Autophagy and Alcohol in Liver Injury.

***Address correspondence to:**
Xiao-Ming Yin, MD, PhD
Department of Pathology and Laboratory Medicine,
Indiana University School of Medicine,
Indianapolis, IN 46202
317-274-1779 (phone)
317-274-1728 (fax)
xmyin@iu.edu (e-mail)

Disclosures: None declared.

Number of pages: 40 **Number of Figures: 7**

Funding: Partially supported by NIH

This is the author's manuscript of the article published in final edited form as:
Yan, S., Zhou, J., Chen, X., Dong, Z., & Yin, X.-M. (2019). Diverse Consequences in Liver Injury in Mice with Different Autophagy Functional Status Treated with Alcohol. The American Journal of Pathology. https://doi.org/10.1016/j.ajpath.2019.05.011

ABSTRACT

Alcoholic fatty liver disease is often complicated by other pathological insults, such as viral infection or high fat diet. Autophagy plays a homeostatic role in the liver but can be compromised by alcohol, high fat diet, or viral infection, which in turn affect the disease process caused by these etiologies. To understand the full impact of autophagy modulation on alcohol-induced liver injury, several genetic models of autophagy deficiency, which have different levels of functional alterations, were examined following acute binge or chronic-plus-binge treatment. Alcohol given in either mode to the liver-specific inducible *Atg7*-deficient mice shortly after the induction of *Atg7* deletion had an elevated liver injury, indicating the protective role of autophagy. Constitutive hepatic *Atg7* deficient mice, in which *Atg7* was deleted in embryos, were more susceptible to chronic-plus-binge but not to acute alcohol treatment. Constitutive hepatic *Atg5* deficient mice, in which *Atg5* was deleted in embryos, were more prone to acute alcohol treatment, but liver injury were surprisingly improved in the chronic-plus-binge regime. A prolonged autophagy deficiency may complicate the hepatic response to alcohol treatment, likely in part due to endogenous liver injury. The complexity of the relationship between autophagy deficiency and alcohol-induced liver injury can thus be affected by the timing of autophagy dysfunction, the exact autophagy gene being affected, and the alcohol treatment regime.

INTRODUCTION

The liver plays a critical role in metabolism in the body [1]. When metabolic homeostasis is disturbed in the liver, fatty liver disease (FLD) can occur, which is characterized by steatosis, inflammation, and fibrosis. FLD can be classified as the one caused by excessive alcohol intake (alcoholic fatty liver disease, AFLD) and the other that is caused by any non-alcohol etiologies (nonalcoholic fatty liver disease, NAFLD) [2].

Autophagy is an evolutionarily conserved cellular degradation process, which involves the delivery of cytoplasmic cargo (macromolecules or organelles) to the lysosome [3]. Three types of autophagy have been defined, ie, macroautophagy, microautophagy, and chaperone-mediated autophagy [4]. Macroautophagy is quantitatively the most active form of autophagy and referred to hereafter as autophagy. In macroautophagy, cytosolic materials are sequestered inside the autophagosome, and transported to and degraded in the lysosome [5]. Autophagy occurs at the basal level in the liver and can be further enhanced under stressed conditions. It can play an important role in the maintenance of normal liver functions and in the pathogenesis of different liver diseases [6, 7]. In particular, autophagy could be activated or depressed in such common liver diseases as AFLD [8, 9, 10, 11, 12], NAFLD [13, 14, 15] and hepatitis virus infection [16-19].

The pathological processes of AFLD are considered to be related to oxidative stress caused by accumulation of acetaldehyde, increase of the NADH/NAD+ ratio, or generation of reactive oxidative species (ROS) [20-22]. Oxidative stress may induce functional and structural changes of mitochondria during the progress of AFLD, which affect oxidative phosphorylation, increase mitochondrial DNA damage, and alter mitochondrial protein profiles [23-28]. Increased reactive oxygen species, together with alcoholic steatosis, lead to lipid peroxidation that can further enhance oxidative damage in AFLD [29]. As shown in previous studies, effects of autophagy can vary at different pathological stages of AFLD. Autophagy is activated in the liver *in vivo* and in

cultured primary hepatocytes after acute alcohol treatment [8, 9 30]. This activation requires alcohol metabolism, and is mediated by reactive oxygen species, and several signaling pathways. Acetaldehyde, a major alcohol metabolite and a pro-oxidant, has been implicated in the induction of autophagy [31]. Meanwhile, alcohol-induced autophagy can be suppressed by anti-oxidants, such as N-acetyl cysteine (NAC) [8, 32]. In addition, alcohol treatment also alters the mammalian target of rapamycin (mTOR), 5' AMP-activated protein kinase (AMPK), and/or Forkhead box O3 (FOXO3a) signaling pathways [33-35], which can contribute to the change of autophagy process. Other autophagy stimulators, including alcohol-induced endoplasmic reticulum (ER) stress, proteasome inhibition, and metal elements such as zinc, are also implicated in the autophagy dynamics following alcohol treatment [36-38].

Interestingly, autophagy may be suppressed in chronic alcohol treatment or in other liver diseases. When mice were fed with Lieber-DeCarli diet for four weeks, hepatic autophagy was stimulated at a lower dose of alcohol (accounting for 29% of the caloric need) but was inhibited at a higher alcohol dose (accounting for 36% of the caloric need) [15]. The suppression of autophagy by long-term alcohol use may suggest that promotion of autophagy can improve the condition. The cause of the autophagy suppression may include the decrease in both the amount and the function of lysosomes, which was found in chronic alcohol-treated rat livers [10, 11, 39]. Indeed, a recent study suggested that the level of transcription factor EB (TFEB), which plays a critical role in lysosomal biogenesis and autophagy, was decreased in the livers of mice given alcohol diet and of patients with alcohol-induced hepatitis [12]. Disruption of hepatic TFEB enhanced alcohol-induced liver injury in mice, but increase of TFEB level led to reduced alcohol-induced liver injury through elevated lysosomal biogenesis and mitochondrial bioenergetics [12].

Nevertheless, the assessment of the contribution of autophagy to alcohol-induced liver injury had been mainly conducted through acute pharmacological manipulation or acute knockdown of

certain autophagy-related genes. The role of autophagy, particularly in the prolonged deficient status, has not been assessed for the impact on alcoholic liver diseases. This may be important as alcohol liver disease is often complicated by other disease-causing factors, such as viral infection or high fat diet, which can compromise autophagy. The present study thus employed several genetic models of autophagy deficiency and assessed the effects of alcohol under different autophagy functional status. The findings suggest that the complicated interaction of alcohol and autophagy in liver injury can be affected by the timing of autophagy dysfunction, the exact autophagy gene being affected, and the alcohol treatment regime.

MATERIALS AND METHODS

Mice

Atg5$^{F/F}$ mice (*B6.129S-Atg5tm1Myok*) [40] and *Atg7*$^{F/F}$ mice [41] have been reported in previous studies. *Atg5*$^{\Delta hep}$ *Atg7*$^{\Delta hep}$ mice were generated by crossing *Atg5*$^{F/F}$ or *Atg7*$^{F/F}$ with the Alb:Cre transgenic mice (The Jackson Laboratory, Bar Harbor, ME), respectively. The liver-specific inducible *Atg7*-deficient mice (*Atg7*$^{\Delta hep\text{-}ERT2}$) were generated by crossing *Atg7*$^{F/F}$ mice to Alb:Cre-ER^{T2} mice [42]. Deletion of *Atg7* was induced by administration of tamoxifen (6 mg/day, x2 days, s.c.). Mice were maintained on a 12-hour dark/12-hour light cycle with free access to food and water. Both male and female mice were used in the studies. Age- and sex-matched mice were randomly assigned to treatment or control group.

Animal models

Acute alcohol binge was conducted as previously described [8]. After six hours of fasting, mice were given 31.5% (vol/vol) alcohol by gavage at a total accumulative dosage of 5 g/kg bodyweight in four equally divided doses in 20 min intervals. For *Atg7*$^{\Delta hep\text{-}ERT2}$ and the control

Atg7$^{F/F}$ mice, they were injected with tamoxifen (6 mg/mouse, s.c. daily x2) 7 days before they were given acute alcohol binge as above or as indicated in the figure legends. The control mice were given the same volume of water.

The chronic-plus-binge model was conducted as previously described [43]. Mice were acclimated with liquid control food for 5 days. The alcohol groups were then given a liquid diet containing 5% (w/v) alcohol for 10 days. Pair-fed groups were given the same volume of control food. In the early morning of day 11, mice in the alcohol groups were given a single dose of 31.5% (vol/vol) alcohol (5 g/kg bodyweight) by gavage. Pair-fed mice were given an isocaloric dose of dextrin maltose by gavage. After nine hours, the mice were euthanized, and blood and tissue samples were collected.

All animal experiments were approved by the Institutional Animal Care and Use Committee (IACUC) of Indiana University.

Antibodies and chemicals

Antibodies and PCR primers used in this study are listed in Table 1 and Table 2, respectively. Tamoxifen (Sigma-Aldrich, St. Louis, MO) were diluted in corn oil. Alcohol (190 proof, Decon Labs, King of Prussia, PA) was diluted in water or added to a formulated liquid diet [43]. Lieber-DeCarli '82 Shake and Pour alcohol liquid diet (Bio-Serv, product no. F1258SP) was used as the alcohol diet. Lieber-DeCarli '82 Shake and Pour control liquid diet (Bio-Serv, product no. F1259SP) was used as the control diet.

Serum biochemistry analysis

Serum levels of alanine aminotransferase (ALT), aspartate aminotransferase (AST), alkaline phosphatase (ALP), triglycerides (TG), and total cholesterol (TCHO) were measured using kits from Pointe Scientific (Canton, MI) according to the manufacturer's protocol. Serum total bile

acids (TBA) were measured using total bile acids assay kit from Diazyme Laboratories, Inc (Poway, CA).

Hepatic lipid content analysis

A piece of liver tissue was weighed and incubated in 1 mL of chloroform-methanol mix (2:1, v/v) with shaking for one hour at room temperature to extract lipids. After addition of 200 µL of water, samples were vortexed and centrifuged at 3,000 × g for 5 minutes. The lower lipid phase was collected and dried at room temperature in a chemical hood. The lipid pellet was re-suspended in 60 µL of tert-butanol and 40 µL of a Triton X-114-methanol (2:1, v/v) mix. Triglycerides and cholesterol contents were measured, using respective kits from Pointe Scientific (Canton, MI). The lipid contents hence were normalized with the tissue weight.

Hepatic TBA content analysis

Liver tissue (100 mg) samples were homogenized in 1 mL of 90% alcohol and incubated at 55 ℃ overnight. The lysates were centrifuged at 10,00 0 rpm for 10 min. The supernatants were collected and measured for total bile acid concentration using total bile acids assay kit from Diazyme Laboratories, Inc (Poway, CA).

Immunoblotting analysis

The liver samples were homogenized in the radio immunoprecipitation assay buffer (RIPA) containing a protease cocktail. Supernatant was collected after centrifuged at 12,000×rpm for 12 min. Protein concentration was determined using BCA protein assay kit (Thermo Fisher Scientific-Pierce). The proteins were separated on a sodium dodecyl sulfate polyacrylamide gel electrophoresis (SDS-PAGE). Proteins were transferred onto polyvinylidene fluoride (PVDF) membranes, which were then blocked with 5% BSA or 5% skim milk for one hour at room temperature. Membranes were incubated with the appropriate primary antibody overnight and

then washed with TBST (Tris-buffered saline, 0.1% Tween 20) before being incubated with the horseradish peroxidase–coupled secondary antibodies at room temperature. Protein bands were detected using enhanced chemiluminescence (ECL) kit (Thermo Fisher Scientific-Pierce). The images were taken digitally with a BioRad ChemiDoc Image System (BioRad, Hercules, CA). Densitometry was measured using the companion software, and the values were normalized to that of β-actin or GAPDH, which were then converted to fold change of the control.

RNA isolation and quantitative real-time PCR analysis

Total RNA was prepared from liver samples using GeneTET RNA purification kit (Thermo Fisher Scientific, Grand Island, NY) according to the manufacturer's protocols. Complementary DNA (cDNA) was synthesized using Oligo dT primers and an M-MLV reverse transcriptase system (Life Technologies-Thermo Fisher Scientific). Quantitative real-time PCR analysis (RT-qPCR) was performed on a 7500 Real-Time PCR System (Life Technologies-Applied Biosystems) using SYBR Green master mixes (Life Technologies-Applied Biosystems). All RT-qPCR results were normalized to the level of β-actin and the gene expression was calculated using the $2^{-\Delta\Delta Ct}$ method.

Histological study

Liver samples were harvested, rinsed with PBS, and fixed in 10% formalin overnight. Samples were further fixed in 70% alcohol and processed as paraffin-embedded blocks. The paraffin-embedded tissues were sectioned and stained with hematoxylin and eosin (H&E), anti-F4/80, or Mason's Trichrome C. Photomicrographs were taken using a Nikon Eclipse E200 light microscope equipped with a SPOT RT Slider color digital camera (Diagnostic Instruments, Inc, Sterling Heights, MI). Area with positive F4/80 or Mason's Trichrome C staining were quantified

using ImageJ software (NIH), at least four random fields of each section from each mouse liver were used for quantification.

Immunofluorescence microscopy

Paraffin sections were subjected to antigen retrieval treatment using the Citrate buffer (0.01M, pH 6.0) after deparaffinization. Slides were blocked with 5% goat serum in PBS containing 0.1% Triton X (PBS-Tx) for one hour and then incubated with primary antibodies diluted in 1% bovine serum albumin (BSA)/PBS-Tx overnight at 4 ℃. Secti ons were washed with PBS, following by incubation with fluorochrome-conjugated secondary antibodies. Hoechst 33342 was used for nucleus staining. Images were obtained using a Nikon Eclipse TE 200 epi-immunofluorescence microscope and the companion NIS-Elements AR3.2 software. Quantification was performed using ImageJ software (NIH), at least four random fields of each section from each mouse liver were analyzed.

Alcohol clearance analysis

Mice were given a single dose of 31.5% (vol/vol) alcohol by gavage (5 g/kg bodyweight). Blood were sampled from the tail vein before the treatment and at 1, 3, and 9 hours after gavage. Alcohol concentration was measured in the plasma using an alcohol colorimetric/fluorometric assay kit (BioVision Inc., Milpitas, CA).

Statistical analysis

Statistical analyses were performed using SPSS for Windows 17.0 Software (SPSS, Inc., Chicago, IL) or Microsoft Excel 2016. Student's *t*-test was used to determine differences between two groups. Differences between more than two treatment groups were determined using one-way analysis of variance (ANOVA) followed by Duncan's post-hoc test. Data were

represented as means with standard errors (mean ± S.E.). Results were considered statistically significant for *P*-value < 0.05.

RESULTS

Genetic deletion of a key autophagy gene enhances liver injury induced by acute alcohol binge

To evaluate the effects of hepatic autophagy deficiency on ALDs, one single binge dose of alcohol was administered to the *Atg5*$^{\Delta hep}$ mice and the control mice (Fig.1A). Hepatic *Atg5* deficiency induced significant hepatomegaly and liver injury (Fig. 1B). Serum levels of ALT, AST, and ALP, and total hepatic TG, but not hepatic cholesterol levels, were further elevated in *Atg5*$^{\Delta hep}$ mice following alcohol treatment (Fig.1B), suggesting that acute alcohol treatment exacerbated the liver pathology in these mice. A protective function of autophagy against hepatic steatosis induced by acute alcohol administration has been shown in several studies [8, 15, 30, 31].

Genetic deletion of *Atg7* in hepatic parenchymal cells caused a more severe liver phenotype than that seen in *Atg5*$^{\Delta hep}$ mice[40] (Fig. 1C). In these mice a single binge dose of alcohol did not further lead to notable increases in serum levels of liver markers and hepatic TG level (Fig.1C). It seemed that a constitute deletion of *Atg7* in hepatic parenchymal cells causes too severe an injury that the relative minor effects of acute alcohol treatment were blunted.

To separate the injury effect caused by constitutive *Atg7* deletion and alcohol treatment, *Atg7*$^{\Delta hep\text{-}ERT2}$ mice were injected with tamoxifen to induce an acute deletion of *Atg7* in the liver before alcohol treatment (Fig. 1D). The deficiency of hepatic autophagy in *Atg7*$^{\Delta hep\text{-}ERT2}$ mice following tamoxifen injection was confirmed by immunoblotting demonstration of decreases in hepatic LC3II/ LC3I ratio and accumulation of SQSTM1/p62 protein (Supplemental Fig S1). Obvious hepatomegaly and serum elevation of liver injury markers in the *Atg7*$^{\Delta hep\text{-}ERT2}$ mice was

not observed in 9 days after induction; however, the serum markers and hepatic TG levels were significantly increased following the acute alcohol treatment in these mice (Fig. 1E). The results were consistent with previous results in which autophagy was modified transiently and acutely using chemicals or gene knockdown [8, 9, 15]. Therefore, an acute deletion of *Atg7,* while not causing liver injury alone*,* rendered the hepatocytes more susceptible to alcohol.

Acute deletion of Atg7 *gene enhances alcohol-induced liver injury in a chronic-plus-binge model*

To further examine the impact of hepatic autophagy deficiency alcohol exposure, the response of these genetically altered mice was analyzed to a more chronic alcohol exposure using a recently established chronic-plus-binge model [43] (Fig. 2A). *Atg7*$^{\Delta hep\text{-}ERT2}$ and *Atg7*$^{F/F}$ mice were given tamoxifen at day 3 and 4 in a 5-day acclimation period, followed by an alcohol diet for 10 days plus an acute alcohol binge at the end of the feeding period. Autophagy deficiency was confirmed as indicated by the reduced level of ATG7 and LC3II/LC3I ratio and an elevated SQSTM1/p62 in the liver of *Atg7*$^{\Delta hep\text{-}ERT2}$ mice (Fig. 2B and C). Consistently, nuclear factor erythroid 2–related factor 2 (NRF2) was activated and its targets, glutathione S-transferase M1 (*Gstm1*) and NAD(P)H quinone dehydrogenase 1 (*Nqo1*), was expressed at a much higher level in the liver of *Atg7*$^{\Delta hep\text{-}ERT2}$ mice (Fig. 2B-2D). Notably, alcohol treatment did not alter these changes due to Atg7 deletion, although it increased the LC3II/LC3I ratio in the floxed normal mice (Fig. 2B-2D).

A longer duration of *Atg7* deletion in the *Atg7*$^{\Delta hep\text{-}ERT2}$ mice resulted in enlarged livers and liver injury in the chronic-plus-binge model (Fig.2E) as compared with the shorter duration of deletion in the binge model (Fig.1E). But as in the binge model, the hepatomegaly and liver injury phenotype (ALT and AST levels), but not that of ALP and TBA, were further augmented by

alcohol treatment (Fig.2F).These results suggested a protective function of *Atg7*-mediated autophagy in alcohol-induced liver injury.

To determine potential factors that promote injury in autophagy deficiency, the extent of steatosis was examined. Hepatic TG (Fig. 2G), but not TCHO (Supplemental Fig. S2A), levels were altered after alcohol treatment, indicating the presence of steatosis in the liver of both *Atg7*$^{F/F}$ and *Atg7*$^{\Delta hep\text{-}ERT2}$ mice but the difference was not significant between the two types of mice. Consistently, alcohol-induced elevation of fatty acid–oxidation as measured by the serum level of β-hydroxybutyrate (β-OHB) was not altered in the absence of Atg7 (Fig. 2G).

Histological examination suggested no obvious differences in general structure and fibrosis, but an elevated presence of Kupffer's cells in autophagy deficient livers (Supplemental Fig. S2B-E). Two acute phase proteins, LCN-2 and SAA2, which are secreted by hepatocytes and other extrahepatic tissues in response to stress or injury, have been recently found to promote alcoholic liver pathology [44, 45]. Indeed, expression of both *LCN2* and *SAA2* were elevated in *Atg7*$^{\Delta hep\text{-}ERT2}$ livers, likely in response to autophagy deficiency–induced stress (Supplemental Fig. S3A). Following the 10-day chronic plus binge alcohol treatment the expression of LCN2 and SAA1 was elevated in floxed-control mice, but not higher than the already elevated level in the Atg7-deficient livers (Supplemental Fig. S3A). In addition, the mRNA levels of several inflammatory cytokines and inflammatory cell markers were higher in alcohol-treated *Atg7*$^{\Delta hep\text{-}ERT2}$ livers than in the same treated floxed mice (Supplemental Fig. S3B-C). But several of them, such as *Ccl2* and *Tlr4*, were also elevated in *Atg7*$^{\Delta hep\text{-}ERT2}$ livers without alcohol treatment. These findings suggest that the protective effect of autophagy may not be entirely related to modulation of inflammation.

Constitutive deletion of hepatic Atg7 exacerbates alcohol-induced liver injury in a chronic-plus-binge model

Chronic alcohol treatment caused more injury than acute binge treatment (Fig 2E vs Fig 1E), which could allow the detection of *Atg7*-mediated protection even in the constitutive deletion model. Thus, *Atg7*$^{\Delta hep}$ and the control mice alcohol were administered diet using the chronic-plus-binge scheme (Fig.3A). As in the inducible *Atg7*$^{\Delta hep\text{-}ERT2}$ mice, alcohol diet did not significantly alter the reduced level of ATG7 and LC3II/ LC3I ratio, and the accumulation of SQSTM1 and NQO1 in the liver of *Atg7*$^{\Delta hep}$ mice (Fig.3B and C). Alcohol enhanced hepatomegaly (Fig. 3D) and liver injury based on the increased serum level of ALT and AST (Fig.3E). There were no significant differences in the serum level of ALP and TBA with or without alcohol treatment (Fig.3E). In addition, total hepatic TG and TCHO levels were increased in *Atg7*-deficient liver by alcohol treatment (Fig.3F). These results indicated that constitutive loss of *Atg7* may exacerbate injury caused by chronic alcohol treatment as well.

Constitutive deletion of hepatic Atg5 does not enhance liver injury in a chronic-plus-binge model

A single dose of alcohol binge treatment enhanced liver injury in *Atg5*$^{\Delta hep}$ mice (Fig.1B). Chronic alcohol treatment of *Atg5*$^{\Delta hep}$ mice (Fig. 4A) did not result in significant alterations in the repression of autophagy in these mice (Fig.4B-D). Alcohol treatment slightly increased hepatomegaly in younger *Atg5*$^{\Delta hep}$ mice (Fig.4E), but significantly decreased the serum levels of ALT, AST, and ALP in both younger and older *Atg5*$^{\Delta hep}$ mice (Fig.4F-H). The reduced injury was observed in both male and female mice (Supplemental Fig. S4A and Supplemental Fig. S5A). Total hepatic TG level but not cholesterol level was still increased in *Atg5*$^{\Delta hep}$ and in *Atg5*$^{F/F}$ mice following alcohol treatment (Fig.4I-4L, Supplemental Fig. S4B, Supplemental Fig. S5B), indicating an expected hepatic response to alcohol. Consistent with a higher level of total hepatic TG in *Atg5*$^{\Delta hep}$ mice following alcohol treatment, hematoxylin and eosin staining of the liver sections also showed a more prominent hepatic steatosis in these mice (Fig.5A).

It is well established that elevation of hepatic TG level is an immediate consequence of alcohol stimulation and steatosis is also a major pathological phenomenon in AFLD [46, 47] . Generally, alcohol can affect hepatic lipid metabolism by accelerating lipogenesis, decelerating lipid breakdown, and causing defective hepatic lipids export[47]. The mRNA expression of several lipid metabolism related–genes in the *Atg5*$^{\Delta hep}$ mice was altered from that in the Atg5$^{F/F}$ mice before and/or after alcohol treatment (Supplemental Fig.S6A-E). Genes involved in lipid secretion, such as apolipoprotein B (*Apob*) and apolipoprotein E (*Apoe*), was reduced, whereas expression of genes involved in lipid update was increased before or after alcohol treatment, such as cluster of differentiation 36 (*Cd36*) and lipoprotein lipase (*Lpl*). Although expression of genes involved in lipogenesis was not elevated, except stearoyl coenzyme A desaturase 1 (*Scd1)*, expression of genes involved in lipolysis, such as adipose triglyceride lipase (*Atgl*) and hormone sensitive lipase E (*Lipe),* and genes in lipid oxidation, such as acyl-CoA dehydrogenase long chain (*Acadl*), acyl-CoA dehydrogenase medium chain (*Acadm*), peroxisomal acyl-coenzyme A oxidase 1 (*Acox1*), and peroxisome proliferator-activated receptor alpha (*Ppar-α*), were repressed. Moreover, expression of genes involved in lipid oxidation was overall reduced in *Atg5*$^{\Delta hep}$ mice (Supplemental Fig. S6E); however, the serum level of β-OHB remained elevated in response to alcohol stimulation (Supplemental Fig. S6F). These changes may overall favor the accumulation of lipids in the cells and decrease lipid use.

The number of F4/80^{+} staining macrophages was significantly increased in *Atg5*$^{\Delta hep}$ livers, similar to what was observed in *Atg7*$^{\Delta hep}$ livers[48]. The level of macrophage expansion was noticeably reduced by alcohol treatment (Fig.5B and C). The expression level of many inflammation-related genes was not significantly altered in *Atg5*-deficient livers, except C-C motif chemokine ligand 2 (*Ccl2*), which was increased in *Atg5*-deficient livers (Supplemental Fig.S7). Alcohol treatment reduced the levels of *Ccl2* and several other cytokines and inflammatory cell markers in these mice (Supplemental Fig.S7A-B). On the other hand, the

expression level of *LCN2* and *SAA2* remained higher (Supplemental Fig. S7C). Inflammation plays important roles in the pathogenesis of ALFD [49]. In particular CCL2 is associated with the severity and neutrophil infiltrates in ALD [50]. Thus, the reduction of inflammation in chronic alcohol treatment condition may contribute to the reduced injury level in *Atg5*$^{\Delta hep}$ livers.

Interestingly, the significantly elevated fibrosis in *Atg5*-deficient livers was also decreased by chronic alcohol treatment as shown by Masson's trichrome staining (Fig.5D and E), hydroxyproline level (Fig. 5F), and the expression of α-smooth muscle actin (α-SMA), at the protein (Fig. 5G) and the mRNA levels (Fig. 5H). Other fibrosis related genes such as connective tissue growth factor (*Ctgf*), transforming growth factor beta 1 (Tgf-β), TIMP metallopeptidase inhibitor 1 (*Timp1*), and glial fibrillary acidic protein (*Gfap*) did not show significant differences between alcohol treatment and control diet (Fig.5H). This improving effect of alcohol is reminiscent of an earlier study showing a potentially protective effect of light alcohol consumption on hepatocellular injury and liver fibrosis in NAFLD patients [51]. It seems that alcohol may have variable effects on hepatic fibrosis under different pathological conditions, which may partially explain the improvement of liver fibrosis in *Atg5*-deficient livers following alcohol treatment.

Reduction in cholestatic injury in Atg5-deficient livers following alcohol treatment

Autophagy deficiency in the liver can cause cholestatic injury, which is accompanied by a significant ductular reaction [48, 52]. Alcohol treatment reduced this pathological change in *Atg5*$^{\Delta hep}$ livers as measured by the level of cytokeratin 19 (CK19) positive ductular cell (Fig.6A and B). Consistently, the serum level of total bile acids (TBA) was also decreased in *Atg5*$^{\Delta hep}$ mice following alcohol treatment in both sexes and at both the older (Fig.6C) and younger ages (Supplemental Fig. S8A). Similar chronic alcohol treatment of *Atg7*$^{\Delta hep\text{-}ERT2}$ (Fig. 2F) or *Atg7*$^{\Delta hep}$ (Fig. 3E) did not reduce the elevated serum TBA levels in these mice. Unexpectedly, the hepatic

TBA load remained high in *Atg5*$^{\Delta hep}$ mice even following alcohol treatment regardless of ages (Fig.6D and E, Supplemental Fig. S8B and C). Interestingly, *Atg5*$^{\Delta hep}$ mice given one dose of alcohol binge also showed a reduced serum bile acid level, in contrast to *Atg7*$^{\Delta hep}$ and *Atg7*$^{\Delta hep\text{-}ERT2}$ mice given the same acute treatment (Supplemental Fig. S8D).

The mRNA levels of genes related to bile acid metabolism were analyzed to determine any potential effects of alcohol. The expression of many of these genes was decreased in *Atg5*-deficient livers as previously reported [52] (Supplemental Fig.S9). However, overall, the mRNA levels of genes related to BAs synthesis were not further significantly altered in *Atg5*-deficient liver following alcohol treatment (Supplemental Fig.S9A-S9B). In addition, the expression of genes related to FXR signaling remained low in *Atg5*-deficient livers (Supplemental Fig.S9C). The impact of autophagy deficiency on the expression of the bile acid transporters was as reported before [52], most of which were not further significantly affected by the alcohol (Supplemental Fig.S9D-S9F). Exceptions were the expression of organic solute transporter beta (Ost-β) in *Atg5*$^{\Delta hep}$ liver (Supplemental Fig.S9E) and that of *Oatp1* in *Atg5*$^{F/F}$ liver (Supplemental Fig.S9F), which were significantly decreased following alcohol treatment. Gene expression results indicated that the influence of alcohol on the bile acid metabolism of *Atg5*-deficient livers would likely be limited.

Hepatic Atg5 deficiency alters the expression of genes related to alcohol metabolism and the plasma alcohol clearance rate in mice

Acetaldehyde along with other alcohol metabolites are considered to be responsible for alcoholic liver diseases [53]. Since alcohol-induced liver injury is affected by alcohol metabolism, it was tested whether alcohol metabolism was affected in *Atg5*-deficient livers. The expression of genes related to alcohol metabolism was analyzed. Notably, the mRNA levels of several alcohol dehydrogenase (ADH) genes, including ADH Class I (*Adh1*), ADH Class III (*Adh5*), ADH Class

IV (*Adh7*), and ADH Class II (*Adh4*), were decreased in *Atg5*-deficient livers (Fig.7A). The expression level of cytochrome P450 family 2 subfamily E member 1 (*Cyp2e1*), and catalase (*Cat*) was also decreased in *Atg5*-deficient livers (Fig.7A). Interestingly, the mRNA level of *Adh1*, *Adh4*, *Adh5*, *Cyp2e1*, and *Cat* was also decreased in livers of *Atg5*$^{F/F}$ mice after alcohol treatment.

The mRNA level of several aldehyde dehydrogenases (ALDHs) in the liver was analyzed. A significant decrease in the mRNA expression levels of *Aldh2*, *Aldh4a1*, *Aldh5a1*, *Aldh7a1*, *Aldh8a1*, and *Aldh9a1* was observed in *Atg5*-deficient livers (Fig.7B). Although alcohol did not seem to cause further changes in expression for most of these genes, it elevated *Aldh1a3* gene expression in *Atg5*-deficient livers, and *Aldh18a1* gene expression in *Atg5*$^{F/F}$ livers (Fig.7B). Expression of several other *Aldh* family members, including *Aldh1a1*, *1a2*, *1b1*, *1l1*, *1l2*, *3a2*, *3b1*, and *6a1* was not significantly changed in livers of *Atg5* deficient mice or upon alcohol treatment (Supplemental Fig.S10).

The protein level of ADH, CYP2E1, and ALDH1/2 were further analyzed. Protein stability of CYP2E1 is critical to its induction by alcohol [54]. The protein level of CYP2E1 and ADH was decreased in older (18 to 24 wk) (Fig.7C and D) and younger (8 to 11 wk) (Supplemental Fig.S11) *Atg5*-deficient livers. However, consistent to previous studies [54], the protein level of CYP2E1 was significantly increased after alcohol treatment in livers of both *Atg5*$^{\Delta hep}$ mice and *Atg5*$^{F/F}$ mice (Fig.7C and D, Supplemental Fig.S9). No consistent changes in ADH or ALDH1/2 in either older (18 to 24 wk) or younger (8 to 1 wk) mice was observed (Fig.7C and D, Supplemental Fig.S9). The gene expression and protein expression data indicated that *Atg5* deficiency in the liver altered expression of genes related to alcohol metabolism; however, alcohol itself did not affect the mRNA level of most of these genes. These changes could result in a lower metabolism of alcohol and therefore a lower level of metabolites of alcohol that are known to be responsible for its toxicity.

The lower metabolism of alcohol might cause a higher plasma alcohol level in the *Atg5*-deficient mice. To examine this possibility, *Atg5*$^{\Delta hep}$ and *Atg5*$^{F/F}$ mice were given a single dose of alcohol by gavage, and the plasma levels of alcohol were measured at different time points (Fig.7E). The plasma alcohol in untreated mice was undetectable. The plasma level of alcohol at 1h after gavage was comparable between *Atg5*$^{\Delta hep}$ and *Atg5*$^{F/F}$ mice, suggesting that there was no difference in the intestinal absorption of alcohol (Fig.7E). Interestingly, plasma levels of alcohol were slightly lower at 3h and dramatically lower at 9h in *Atg5*$^{\Delta hep}$ mice than those in *Atg5*$^{F/F}$ mice (Fig.7E). These results indicated an increased plasma alcohol clearance in *Atg5*$^{\Delta hep}$ mice despite a reduction in the expression of genes in the alcohol metabolism pathway. Other mechanisms may therefore account for the alcohol elimination in the autophagy deficient mice.

DISCUSSION

The effect of autophagy on alcohol-induced liver injury is affected by how autophagy is inhibited and how alcohol is administered

This is the first study in which the role of autophagy in alcohol-induced liver injury was assessed through a genetic approach to disrupt the formation of autophagosomes using either inducible or constitutive knockout of two different autophagy genes, *Atg7* and *Atg5*. These models differ in the duration of autophagy deficiency, the specific gene being affected, and the severity of endogenous liver injury. This study thus allows an extensive analysis of the interaction of alcohol administration and autophagy function in the context of acute and chronic liver injury.

Previous studies had examined the role of autophagy by using siRNA-mediated knockdown of *Atg7*, or by interference of the lysosomal functions with chloroquine or TFEB [8, 9, 12, 15, 31]. In these studies, the protective role of autophagy in alcohol-induced liver injury had been shown in the

models of an acute binge, a chronic 4-week Liber-DeCarli feeding, and a chronic-plus-binge feeding. The protective effects of autophagy in the gastric infusion model had also been observed with the use of chloroquine (Zhou and Yin, unpublished observations). In the infusion model alcohol (up to 37.1% of calorie uptake) was given in either a 8% low fat or 40% high fat base over a period of 28 days[55]. Administration of chloroquine led to increased hepatic TG and blood ALT.

Here we have confirmed the protective effect of autophagy in the inducible *Atg7*-deficient livers (*Atg7*$^{\Delta hep\text{-}ERT2}$) using both the acute binge model and a new chronic-plus-binge model. In both models autophagy deficiency via Atg7 deletion was induced only shortly before alcohol treatment. The inducible approach minimized the liver injury caused by autophagy deficiency alone so that the impact of autophagy deficiency on alcohol-induced injury can be directly examined. However, mice harboring constitutive deletion of *Atg7* (*Atg7*$^{\Delta hep}$) had different responses to alcohol treatment in the acute binge and chronic-plus-binge models. Liver injury was noticeably enhanced in *Atg7*$^{\Delta hep}$ mice following the chronic-plus-binge treatment, but not following acute binge treatment. The difference in the liver injury following alcohol treatments between the two Atg7 deletion models may be due to the difference in the duration of gene deletion, which would result in varying levels of autophagy dysfunction and liver injury. It is possible that a higher level of detrimental SQSTM1/p62 accumulation and NRF2 activation *Atg7*$^{\Delta hep}$ mice (Fig. 3B-C vs Fig. 2B-C) may account for this resistance.

For mice with constitutive *Atg5* deletion in the liver (*Atg5*$^{\Delta hep}$), liver injury was noticeably enhanced following a single dose of binge treatment, but paradoxically improved following the chronic-plus-binge treatment. In the latter, the improved presentation included a lower blood level of liver enzymes and total bile acids and a reduced hepatic inflammation, ductular reaction, and fibrosis. It is possible that the level of NRF2 activation could be in part responsible for the difference between the *Atg5*$^{\Delta hep}$ and *Atg7*$^{\Delta hep}$ mice. Thus the levels of SQSTM1/p62 and NQO1

were higher in the Atg7$^{\Delta Hep}$ liver than in the Atg5$^{\Delta Hep}$ livers (Fig. 3B-C vs Fig. 4B-C). The extent of NRF2 activation may determine the severity of endogenous injury [41, 48, 56], which in turn affect the response to alcohol treatment.

These results demonstrate that the outcomes of the interaction of alcohol and hepatic autophagy function could depend on how autophagy function is disabled, constitutively or acutely, which autophagy gene is deleted, *Atg7* or *Atg5*, and how alcohol is administrated. However, published and current results clearly demonstrate that acute inactivation of autophagy or lysosome function, via genetic, chemical (siRNA), or pharmacological approach, promotes alcohol-induced liver injury in a variety of alcohol administration models with different dosages and durations. But the more complex findings of alcohol-induced phenotypes in chronic autophagy deficient mice perhaps more realistically reflect clinical scenarios in which autophagy functions could be compromised through a more chronic process by alcohol and other co-existing factors such as viral infection [16-19] or high fat diet [13, 14, 15].

The variable liver pathology in *Atg5*$^{\Delta hep}$ and *Atg7*$^{\Delta hep}$ mice may contribute to their differential responses to alcohol given through different regimes

Embryonic deletion of Atg5 or Atg7 in the parenchymal cells under the albumin promotor leads to severe liver pathology [48, 56]. Both Atg7 and Atg5 are critical for LC3 to conjugate to phosphatidylalcoholamine (PE) on the autophagosomal membrane, which is required for autophagosome formation. However, the hepatic phenotypes of *Atg5*$^{\Delta hep}$ and *Atg7*$^{\Delta hep}$ mice are interestingly different in the degree and progression of the injury. Overall *Atg5*$^{\Delta hep}$ mice seemed to present a less severe phenotype of liver injury (Fig. 1B-1C). Similar observations could be found in earlier sudies [48, 56]. In addition, *Atg5*-deficient mice seem to undergo a spontaneous improvement when they became older (four months and beyond) (Fig. 4F-H and [56]). Also, the improvement was mainly contributed by the male mice (Supplemental Fig S4A), not the female

mice (Supplemental Fig. S5A). The mechanisms for the more severe phenotype of *Atg7*$^{\Delta hep}$ mice are not clear, but may be related to the more critical function of ATG7 being the only E1-like molecule responsible for both ATG5-ATG12 conjugation and LC3-PE conjugation [5]. Alternatively, the possibility that ATG7 might have additional functions cannot be ruled out.

The mild liver injury associated with Atg5-deficiency could allow the detection of the added alcohol-induced insults in the acute binge model (Fig. 1B). On the other hand, *Atg7*$^{\Delta hep}$ mice might have a blunted response to an acute alcohol binge, and failed to show an increased injury. Since the elevation of hepatic TG level is an immediate consequence of alcohol stimulation and steatosis is a major pathological phenomenon in AFLD.[46, 47], the change in the hepatic total TG level was examined in *Atg7*$^{\Delta hep}$ and *Atg5*$^{\Delta hep}$ mice. Indeed, TG level was not elevated in *Atg7*$^{\Delta hep}$ (Fig. 1C) but was elevated in *Atg5*$^{\Delta hep}$ (Fig. 1B) mice receiving an acute binge treatment. This observation supported that *Atg7*$^{\Delta hep}$ mice had a blunted response to acute alcohol stimulation. In the chronic-plus-binge regime, *Atg7*$^{\Delta hep}$ mice responded to the prolonged alcohol stimulation since the total TG level was elevated (Fig. 3E), and consequently an elevated injury was observed (Fig. 3D).

The response of *Atg5*$^{\Delta hep}$ mice to the chronic-plus-binge treatment was unexpected. The liver injury phenotypes was paradoxically reduced in these mice despite that they seemed to respond to alcohol as evidenced by elevated hepatic TG level (Fig. 4I-J). The improvement in liver injury despite an elevation in hepatic TG was evident in both sexes and regardless the age (Supplemental Fig. S4 and Supplemental Fig. S5). An earlier study had also shown that *Atg5*$^{\Delta hep}$ mice were paradoxically resistant to acetaminophen-induced liver injury as well [57]. A common feature of alcohol- and acetaminophen-induced liver injury is the induction of oxidative stress. Thus it is possible that *Atg5*$^{\Delta hep}$ mice had pathological changes that render them to be resistant to oxidative stress.

Deletion of either *Atg5* or *Atg7* in the liver causes SQSTM1/p62 accumulation in the liver, which in turn activates NRF2 [40, 41, 56, 58]. The latter may create a somewhat reduced environment to resist damages caused by oxidative stress [57]. However, the elevated NRF2 activation in autophagy deficiency is in fact correlated with the pathology as co-deletion of NRF2 blocked most of the liver phenotypes in *Atg7*$^{\Delta hep}$ and *Atg5*$^{\Delta hep}$ mice[41, 48, 56]. Thus the improved hepatic presentation of *Atg5*$^{\Delta hep}$ mice given chronic-plus-binge alcohol treatment may be due to other factors.

The effect of alcohol in mice with chronic liver injury due to autophagy deficiency is thus complicated by the baseline liver changes in autophagy deficient condition. It thus has to be cautious in reaching conclusive remarks on the potential mechanisms that are involved. Notably, clinically alcoholic liver disease is often complicated by other conditions such as viral infection[16-19] and NAFLD[13, 14, 15], both of which could compromise autophagy functions. Long-term alcohol use can also suppress autophagy by itself [9, 10, 11, 12, 15]. This study demonstrated that the effects of alcohol can be quite diverse in livers with a varying degree of autophagy deficiency.

Improvement of liver injury in *Atg5*$^{\Delta hep}$ mice by chronic alcohol treatment may be related to multiple factors

Other factors to consider include the potential role of inflammation, which is known to play important roles in the pathogenesis of ALFD [49,50]. The reduced injury in *Atg5*$^{\Delta hep}$ livers by the chronic alcohol treatment may be related to reduced Inflammation. In addition, changes related to metabolism of bile acids and alcohol itself may deserve attentions as well.

As previously piblished[52, 56], *Atg5*$^{\Delta hep}$ and *Atg7*$^{\Delta hep}$ mice develop cholestatic injury, which is accompanied with increased level of CK19-positive ductular cells (ductular reaction), altered mRNA level of genes in the bile acid metabolism pathways, and an increase of circulating TBA

level. Interestingly, several studies showed a relationship between alcohol administration and BA metabolism [59-61]. Indeed, serum level of TBA was decreased by alcohol treatment in both *Atg5*$^{F/F}$ and *Atg5*$^{\Delta hep}$ mice. However, the improving effect in *Atg5*$^{\Delta hep}$ mice by alcohol may not be related to intrahepatic BA metabolism since the hepatic BA level in *Atg5*$^{\Delta hep}$ remained high (Fig.6D-6E) and the expression of genes that are related to BA metabolism did not change significantly (Supplemental Fig.S9). Nevertheless, this reduction in serum TBA may still be beneficial as suggested by the decrease in ductular reaction (Fig.6A) and serum ALT/AST (Fig.4F-4G). How chronic alcohol treatment and *Atg5*-deficiency lead to improved cholestatic outcome is an interesting topic for future studies.

Alcohol is generally metabolized in hepatic parenchymal cells, which express the highest levels of alcohol-oxidizing enzymes, including ADHs, CYP2E1, and CAT [46]. The first step of alcohol breakdown in the liver by these enzymes generates toxic metabolites, including acetaldehyde and other potentially damaging molecules [53]. Interestingly, the mRNA level of ADHs, *Cyp2e1*, and Cat genes was decreased in *Atg5*-deficient livers. Reduced levels of these alcohol oxidizing enzymes may reduce the generation of toxic metabolites, and thus less or no alcohol-mediated toxicity. However, there was no consistent difference in the expression of these genes between *Atg5*$^{\Delta hep}$ livers and *Atg7*$^{\Delta hep}$ livers (data not shown), which may thus not account for the difference in how these mice responded to alcohol.

The toxic acetaldehyde can be enzymatically removed by acetaldehyde dehydrogenase (Aldh). *Aldh2* is one of the most important Aldh family genes for alcohol metabolism. Either pharmacological activation of *Aldh2* or global *Aldh2* overexpression seem to ameliorate chronic alcohol-induced hepatic steatosis and improved ALD [62, 63]. *Aldh2* deficiency paradoxically resulted in improve alcoholic fatty livers although worsen liver inflammation and fibrosis [64]. The expression of several Aldh genes, including *Aldh2*, was decreased in *Atg5*-deficient livers although the protein level remained unchanged. The significance of this change is not known,

but the overall findings would suggest that alcohol metabolism might be altered in *Atg5*$^{\Delta hep}$ livers, which may contribute to the observed phenotypes.

A lower expression of these enzymes may result in a slower blood alcohol clearance, as in *Adh1* and *Adh4* knockout mice [65]. Surprisingly, a faster clearance rate of plasma alcohol in *Atg5*$^{\Delta hep}$ mice was observed. It is notable that alcohol could be cleared from circulation by other mechanisms independent of these enzymes, such as through breath. The potential involvement of these independent mechanisms needs to be investigated in the future.

In summary, this study has demonstrated a protective role of autophagy in alcohol-induced liver injury, which was best illustrated in models where an autophagy gene, *Atg7*, is acutely deleted. In mice with constitutive deletion of *Atg7* or *Atg5*, the impacts of autophagy deficiency on alcohol-induced liver phenotype become complicated, in large part due to the co-existence of liver pathology caused by autophagy deficiency. Collectively, this study indicates the complexity of the relationship between autophagy status and alcohol-induced liver injury. This relationship is dictated by the timing of the autophagy inhibition and alcohol exposure, the regime of alcohol administration, and the particular autophagy gene being inactivated. These conditions may draw some similarities to the clinical alcoholic liver diseases, which is often complicated by additional confounding factors, such as viral infection[16-19] and NAFLD[13, 14, 15], in which autophagy function can be compromised. This study may provide a model to understand the complex interactions of alcohol with autophagy deficiency at various degrees caused by other underlying conditions.

REFERENCES

[1] Abdel-Misih SR, Bloomston M: Liver anatomy. Surg Clin North Am 2010, 90:643-53.

[2] Reddy JK, Rao MS: Lipid metabolism and liver inflammation. II. Fatty liver disease and fatty acid oxidation. Am J Physiol Gastrointest Liver Physiol 2006, 290:G852-8.

[3] Deter RL, De Duve C: Influence of glucagon, an inducer of cellular autophagy, on some physical properties of rat liver lysosomes. J Cell Biol 1967, 33:437-49.

[4] Meijer AJ, Codogno P: Regulation and role of autophagy in mammalian cells. The international journal of biochemistry & cell biology 2004, 36:2445-62.

[5] Mizushima N, Komatsu M: Autophagy: renovation of cells and tissues. Cell 2011, 147:728-41.

[6] Yin XM, Ding WX, Gao W: Autophagy in the liver. Hepatology 2008, 47:1773-85.

[7] Czaja MJ, Ding WX, Donohue TM, Jr., Friedman SL, Kim JS, Komatsu M, Lemasters JJ, Lemoine A, Lin JD, Ou JH, Perlmutter DH, Randall G, Ray RB, Tsung A, Yin XM: Functions of autophagy in normal and diseased liver. Autophagy 2013, 9:1131-58.

[8] Ding WX, Li M, Chen X, Ni HM, Lin CW, Gao W, Lu B, Stolz DB, Clemens DL, Yin XM: Autophagy reduces acute ethanol-induced hepatotoxicity and steatosis in mice. Gastroenterology 2010, 139:1740-52.

[9] Thomes PG, Trambly CS, Thiele GM, Duryee MJ, Fox HS, Haorah J, Donohue TM, Jr.: Proteasome activity and autophagosome content in liver are reciprocally regulated by ethanol treatment. Biochemical and biophysical research communications 2012, 417:262-7.

[10] Kharbanda KK, McVicker DL, Zetterman RK, Donohue TM, Jr.: Ethanol consumption alters trafficking of lysosomal enzymes and affects the processing of procathepsin L in rat liver. Biochim Biophys Acta 1996, 1291:45-52.

[11] Dolganiuc A, Thomes PG, Ding WX, Lemasters JJ, Donohue TM, Jr.: Autophagy in alcohol-induced liver diseases. Alcohol Clin Exp Res 2012, 36:1301-8.

[12] Chao X, Wang S, Zhao K, Li Y, Williams JA, Li T, Chavan H, Krishnamurthy P, He XC, Li L, Ballabio A, Ni HM, Ding WX: Impaired TFEB-mediated Lysosome Biogenesis and Autophagy Promote Chronic Ethanol-induced Liver Injury and Steatosis in Mice. Gastroenterology 2018.
[13] Yang L, Li P, Fu S, Calay ES, Hotamisligil GS: Defective hepatic autophagy in obesity promotes ER stress and causes insulin resistance. Cell Metab 2010, 11:467-78.
[14] Zhang H, Yan S, Khambu B, Ma F, Li Y, Chen X, Martina JA, Puertollano R, Li Y, Chalasani N, Yin XM: Dynamic MTORC1-TFEB feedback signaling regulates hepatic autophagy, steatosis and liver injury in long-term nutrient oversupply. Autophagy 2018, 14:1779-95.
[15] Lin CW, Zhang H, Li M, Xiong X, Chen X, Chen X, Dong XC, Yin XM: Pharmacological promotion of autophagy alleviates steatosis and injury in alcoholic and non-alcoholic fatty liver conditions in mice. J Hepatol 2013, 58:993-9.
[16] Tang H, Da L, Mao Y, Li Y, Li D, Xu Z, Li F, Wang Y, Tiollais P, Li T, Zhao M: Hepatitis B virus X protein sensitizes cells to starvation-induced autophagy via up-regulation of beclin 1 expression. Hepatology 2009, 49:60-71.
[17] Liu B, Fang M, Hu Y, Huang B, Li N, Chang C, Huang R, Xu X, Yang Z, Chen Z, Liu W: Hepatitis B virus X protein inhibits autophagic degradation by impairing lysosomal maturation. Autophagy 2014, 10:416-30.
[18] Sir D, Chen WL, Choi J, Wakita T, Yen TS, Ou JH: Induction of incomplete autophagic response by hepatitis C virus via the unfolded protein response. Hepatology 2008, 48:1054-61.
[19] Kim SJ, Khan M, Quan J, Till A, Subramani S, Siddiqui A: Hepatitis B virus disrupts mitochondrial dynamics: induces fission and mitophagy to attenuate apoptosis. PLoS pathogens 2013, 9:e1003722.
[20] Lumeng L, Crabb DW: Alcoholic liver disease. Curr Opin Gastroenterol 2000, 16:208-18.
[21] Lieber CS: Alcoholic fatty liver: its pathogenesis and mechanism of progression to inflammation and fibrosis. Alcohol 2004, 34:9-19.

[22] Zakhari S, Li TK: Determinants of alcohol use and abuse: Impact of quantity and frequency patterns on liver disease. Hepatology 2007, 46:2032-9.
[23] Bailey SM, Cunningham CC: Contribution of mitochondria to oxidative stress associated with alcoholic liver disease. Free Radic Biol Med 2002, 32:11-6.
[24] Demeilliers C, Maisonneuve C, Grodet A, Mansouri A, Nguyen R, Tinel M, Letteron P, Degott C, Feldmann G, Pessayre D, Fromenty B: Impaired adaptive resynthesis and prolonged depletion of hepatic mitochondrial DNA after repeated alcohol binges in mice. Gastroenterology 2002, 123:1278-90.
[25] Mansouri A, Demeilliers C, Amsellem S, Pessayre D, Fromenty B: Acute ethanol administration oxidatively damages and depletes mitochondrial dna in mouse liver, brain, heart, and skeletal muscles: protective effects of antioxidants. J Pharmacol Exp Ther 2001, 298:737-43.
[26] Mansouri A, Gaou I, De Kerguenec C, Amsellem S, Haouzi D, Berson A, Moreau A, Feldmann G, Letteron P, Pessayre D, Fromenty B: An alcoholic binge causes massive degradation of hepatic mitochondrial DNA in mice. Gastroenterology 1999, 117:181-90.
[27] Cahill A, Cunningham CC, Adachi M, Ishii H, Bailey SM, Fromenty B, Davies A: Effects of alcohol and oxidative stress on liver pathology: the role of the mitochondrion. Alcohol Clin Exp Res 2002, 26:907-15.
[28] Cahill A, Stabley GJ, Wang X, Hoek JB: Chronic ethanol consumption causes alterations in the structural integrity of mitochondrial DNA in aged rats. Hepatology 1999, 30:881-8.
[29] Wang L, Khambu B, Zhang H, Yin XM: Autophagy in alcoholic liver disease, self-eating triggered by drinking. Clin Res Hepatol Gastroenterol 2015, 39 Suppl 1:S2-6.
[30] Wang L, Zhou J, Yan S, Lei G, Lee CH, Yin XM: Ethanol-triggered Lipophagy Requires SQSTM1 in AML12 Hepatic Cells. Sci Rep 2017, 7:12307.

[31] Thomes PG, Ehlers RA, Trambly CS, Clemens DL, Fox HS, Tuma DJ, Donohue TM: Multilevel regulation of autophagosome content by ethanol oxidation in HepG2 cells. Autophagy 2013, 9:63-73.

[32] Wu D, Wang X, Zhou R, Yang L, Cederbaum AI: Alcohol steatosis and cytotoxicity: the role of cytochrome P4502E1 and autophagy. Free Radic Biol Med 2012, 53:1346-57.

[33] Sid B, Verrax J, Calderon PB: Role of AMPK activation in oxidative cell damage: Implications for alcohol-induced liver disease. Biochem Pharmacol 2013, 86:200-9.

[34] Ding WX, Li M, Yin XM: Selective taste of ethanol-induced autophagy for mitochondria and lipid droplets. Autophagy 2011, 7:248-9.

[35] Ni HM, Du K, You M, Ding WX: Critical role of FoxO3a in alcohol-induced autophagy and hepatotoxicity. Am J Pathol 2013, 183:1815-25.

[36] Ding WX, Yin XM: Sorting, recognition and activation of the misfolded protein degradation pathways through macroautophagy and the proteasome. Autophagy 2008, 4:141-50.

[37] Ding WX, Ni HM, Gao W, Yoshimori T, Stolz DB, Ron D, Yin XM: Linking of autophagy to ubiquitin-proteasome system is important for the regulation of endoplasmic reticulum stress and cell viability. Am J Pathol 2007, 171:513-24.

[38] Liuzzi JP, Yoo C: Role of zinc in the regulation of autophagy during ethanol exposure in human hepatoma cells. Biol Trace Elem Res 2013, 156:350-6.

[39] Kharbanda KK, McVicker DL, Zetterman RK, MacDonald RG, Donohue TM, Jr.: Flow cytometric analysis of vesicular pH in rat hepatocytes after ethanol administration. Hepatology 1997, 26:929-34.

[40] Takamura A, Komatsu M, Hara T, Sakamoto A, Kishi C, Waguri S, Eishi Y, Hino O, Tanaka K, Mizushima N: Autophagy-deficient mice develop multiple liver tumors. Genes Dev 2011, 25:795-800.

[41] Komatsu M, Kurokawa H, Waguri S, Taguchi K, Kobayashi A, Ichimura Y, Sou YS, Ueno I, Sakamoto A, Tong KI, Kim M, Nishito Y, Iemura S, Natsume T, Ueno T, Kominami E, Motohashi

H, Tanaka K, Yamamoto M: The selective autophagy substrate p62 activates the stress responsive transcription factor Nrf2 through inactivation of Keap1. Nat Cell Biol 2010, 12:213-23.

[42] Schuler M, Dierich A, Chambon P, Metzger D: Efficient temporally controlled targeted somatic mutagenesis in hepatocytes of the mouse. Genesis 2004, 39:167-72.

[43] Bertola A, Mathews S, Ki SH, Wang H, Gao B: Mouse model of chronic and binge ethanol feeding (the NIAAA model). Nat Protoc 2013, 8:627-37.

[44] Hu M, Yin H, Mitra MS, Liang X, Ajmo JM, Nadra K, Chrast R, Finck BN, You M: Hepatic-specific lipin-1 deficiency exacerbates experimental alcohol-induced steatohepatitis in mice. Hepatology 2013, 58:1953-63.

[45] Wieser V, Tymoszuk P, Adolph TE, Grander C, Grabherr F, Enrich B, Pfister A, Lichtmanegger L, Gerner R, Drach M, Moser P, Zoller H, Weiss G, Moschen AR, Theurl I, Tilg H: Lipocalin 2 drives neutrophilic inflammation in alcoholic liver disease. J Hepatol 2016, 64:872-80.

[46] Osna NA, Donohue TM, Kharbanda KK: Alcoholic Liver Disease: Pathogenesis and Current Management. Alcohol Res-Curr Rev 2017, 38:147-61.

[47] Sozio M, Crabb DW: Alcohol and lipid metabolism. American Journal of Physiology-Endocrinology and Metabolism 2008, 295:E10-E6.

[48] Khambu B, Huda N, Chen X, Antoine DJ, Li Y, Dai G, Kohler UA, Zong WX, Waguri S, Werner S, Oury TD, Dong Z, Yin XM: HMGB1 promotes ductular reaction and tumorigenesis in autophagy-deficient livers. J Clin Invest 2018, 128:2419-35.

[49] Wang HJ, Gao B, Zakhari S, Nagy LE: Inflammation in alcoholic liver disease. Annu Rev Nutr 2012, 32:343-68.

[50] Degre D, Lemmers A, Gustot T, Ouziel R, Trepo E, Demetter P, Verset L, Quertinmont E, Vercruysse V, Le Moine O, Deviere J, Moreno C: Hepatic expression of CCL2 in alcoholic liver

disease is associated with disease severity and neutrophil infiltrates. Clin Exp Immunol 2012, 169:302-10.

[51] Yamada K, Mizukoshi E, Seike T, Horii R, Kitahara M, Sunagozaka H, Arai K, Yamashita T, Honda M, Kaneko S: Light alcohol consumption has the potential to suppress hepatocellular injury and liver fibrosis in non-alcoholic fatty liver disease. PLoS One 2018, 13:e0191026.

[52] Khambu B, Li T, Yan S, Yu C, Chen X, Goheen M, Li Y, Lin J, Cummings OW, Lee YA, Friedman S, Dong Z, Feng GS, Wu S, Yin XM: Hepatic Autophagy Deficiency Compromises FXR Functionality and Causes Cholestatic Injury. Hepatology 2018.

[53] Lieber CS: Relationships between nutrition, alcohol use, and liver disease. Alcohol Res Health 2003, 27:220-31.

[54] Roberts BJ, Song BJ, Soh Y, Park SS, Shoaf SE: Ethanol induces CYP2E1 by protein stabilization. Role of ubiquitin conjugation in the rapid degradation of CYP2E1. J Biol Chem 1995, 270:29632-5.

[55] Ueno A, Lazaro R, Wang PY, Higashiyama R, Machida K, Tsukamoto H: Mouse intragastric infusion (iG) model. Nat Protoc 2012, 7:771-81.

[56] Ni HM, Woolbright BL, Williams J, Copple B, Cui W, Luyendyk JP, Jaeschke H, Ding WX: Nrf2 promotes the development of fibrosis and tumorigenesis in mice with defective hepatic autophagy. J Hepatol 2014, 61:617-25.

[57] Ni HM, Boggess N, McGill MR, Lebofsky M, Borude P, Apte U, Jaeschke H, Ding WX: Liver-specific loss of Atg5 causes persistent activation of Nrf2 and protects against acetaminophen-induced liver injury. Toxicol Sci 2012, 127:438-50.

[58] Komatsu M, Waguri S, Ueno T, Iwata J, Murata S, Tanida I, Ezaki J, Mizushima N, Ohsumi Y, Uchiyama Y, Kominami E, Tanaka K, Chiba T: Impairment of starvation-induced and constitutive autophagy in Atg7-deficient mice. J Cell Biol 2005, 169:425-34.

[59] Hartmann P, Hochrath K, Horvath A, Chen P, Seebauer CT, Llorente C, Wang L, Alnouti Y, Fouts DE, Starkel P, Loomba R, Coulter S, Liddle C, Yu RT, Ling L, Rossi SJ, DePaoli AM,

Downes M, Evans RM, Brenner DA, Schnabl B: Modulation of the intestinal bile acid/farnesoid X receptor/fibroblast growth factor 15 axis improves alcoholic liver disease in mice. Hepatology 2017.

[60] Hu X, Jogasuria A, Wang J, Kim C, Han Y, Shen H, Wu J, You M: MitoNEET Deficiency Alleviates Experimental Alcoholic Steatohepatitis in Mice by Stimulating Endocrine Adiponectin-Fgf15 Axis. J Biol Chem 2016, 291:22482-95.

[61] Wang J, Kim C, Jogasuria A, Han Y, Hu X, Wu J, Shen H, Chrast R, Finck BN, You M: Myeloid Cell-Specific Lipin-1 Deficiency Stimulates Endocrine Adiponectin-FGF15 Axis and Ameliorates Ethanol-Induced Liver Injury in Mice. Sci Rep 2016, 6:34117.

[62] Zhong W, Zhang W, Li Q, Xie G, Sun Q, Sun X, Tan X, Sun X, Jia W, Zhou Z: Pharmacological activation of aldehyde dehydrogenase 2 by Alda-1 reverses alcohol- induced hepatic steatosis and cell death in mice. Journal of Hepatology 2015, 62:1375-81.

[63] Guo R, Xu X, Babcock SA, Zhang Y, Ren J: Aldehyde dedydrogenase-2 plays a beneficial role in ameliorating chronic alcohol-induced hepatic steatosis and inflammation through regulation of autophagy. J Hepatol 2015, 62:647-56.

[64] Kwon HJ, Won YS, Park O, Chang BX, Duryee MJ, Thiele GE, Matsumoto A, Singh S, Abdelmegeed MA, Song BJ, Kawamoto T, Vasiliou V, Thiele GM, Gao B: Aldehyde Dehydrogenase 2 Deficiency Ameliorates Alcoholic Fatty Liver but Worsens Liver Inflammation and Fibrosis in Mice. Hepatology 2014, 60:146-57.

[65] Deltour L, Foglio MH, Duester G: Metabolic deficiencies in alcohol dehydrogenase Adh1, Adh3, and Adh4 null mutant mice. Overlapping roles of Adh1 and Adh4 in ethanol clearance and metabolism of retinol to retinoic acid. J Biol Chem 1999, 274:16796-801.

FIGURE LEGENDS

Fig. 1 Genetic deletion of autophagy genes exacerbates liver injury induced by acute alcohol binge. A: Scheme of acute binge treatment. Mice were treated with a single dose of alcohol or the same volume of distilled water by gavage after six hours of fasting. Mice were euthanized 16 hours later. **B-C:** Liver weight and body weight ratio (%), the serum levels of ALT, AST, ALP, and the hepatic levels of triglycerides (TG) and total cholesterol (TCHO) were measured in liver-specific *Atg5* (**B**, 8 to 34 wk old, n=7 to 14) and *Atg7* (**C**, 8 to 16 wk old, n=3 to 6) deficient mice. **D:** Scheme of the administration of alcohol to $Atg7^{\Delta hep\text{-}ERT2}$ mice. Tamoxifen (TMX) was injected at day 1 and day 2 to induce the deletion of *Atg7*. Alcohol or water was then given by oral gavage on day 8. $Atg7^{F/F}$ mice were used as control. **E:** Liver weight and body weight ratio (%), the serum levels of ALT, AST, ALP, and the hepatic levels of TG and TCHO were measured in induced $Atg7^{\Delta hep\text{-}ERT2}$ mice (8 to 15 wk old, n=3 to 5). **P* < 0.05 versus non-treated F/F control; †*P* < 0.05 versus non-treated ΔHep control, ‡ *P* < 0.05 versus treated F/F control.

Fig.2 Acute deletion of *Atg7* enhances alcohol-induced liver injury in a chronic-plus-binge model. A: Scheme of the chronic-plus-binge treatment. Mice were acclimatized with liquid diet for 5 days. $Atg7^{F/F}$ and $Atg7^{\Delta hep\text{-}ERT2}$ mice were injected with TMX at day 3 and day 4 during acclimatization. After acclimatization, mice were randomly divided into two groups and given a liquid diet with alcohol (EtOH-fed) or with maltose dextrin (Pair-fed) for 10 days, followed by a single gavage of alcohol (5g/kg) or iso-caloric maltose dextrin. Mice were analyzed nine hours later. **B:** Representative western blot images of protein expression in the livers of $Atg7^{F/F}$ and $Atg7^{\Delta hep\text{-}ERT2}$ mice following alcohol or pair-fed treatment. *non-specific bands. **C:** Densitometry of each protein band was conducted. The density of ATG7, P62, or NQO1 was normalized to that of β-Actin. The density of LC3II was normalized to that of LC3I. These values were expressed as fold change over those of pair-fed $Atg7^{F/F}$ mice (n=4). **D:** The mRNA level of

Gstm1 and *Nqo1* in the livers of *Atg7*$^{F/F}$ and *Atg7*$^{\Delta hep\text{-}ERT2}$ mice following alcohol or pair-fed treatment. Expression levels were normalized to that of β-Actin and expressed as the fold change over those of pair-fed *Atg7*$^{F/F}$ (n=4). **E-F:** Liver weight and body weight ratio (%), serum levels of ALT, AST, ALP, and TBA in *Atg7*$^{F/F}$ and *Atg7*$^{\Delta hep\text{-}ERT2}$ mice following alcohol or pair-fed treatment. **G:** Hepatic TG and serum β-hydroxybutyrate (β-OHB) levels in *Atg7*$^{F/F}$ and *Atg7*$^{\Delta hep\text{-}ERT2}$ mice given alcohol or pair-fed treatment. Mice were used at the age of 8 to 12 wk, n=4 to 11. *Gstm1*: glutathione S-transferase M1, and *Nqo1*: NAD(P)H quinone dehydrogenase 1 (Nqo1). **P* < 0.05 versus non-treated F/F control; †*P* < 0.05 versus non-treated ΔHep control, ‡*P* < 0.05 versus treated F/F control.

Fig.3 Constitutive deletion of hepatic *Atg7* enhances alcohol-induced liver injury in a chronic-plus-binge model. A: Scheme of the chronic-plus-binge treatment. *Atg7*$^{F/F}$ and *Atg7*$^{\Delta hep}$ mice were acclimatized with liquid diet for five days. After acclimatization, mice were randomly divided into two groups and given alcohol or control diet as in Fig.2. **B:** Representative western blot images of protein expression in the liver from *Atg7*$^{F/F}$ and *Atg7*$^{\Delta hep}$ mice following alcohol or pair-fed treatment. SE: short exposure; LE: long exposure. **C:** The density of ATG7, P62, or NQO1 was normalized to that of GAPDH. The density of LC3II was normalized to that of LC3I. These values were expressed as fold change over those of pair-fed *Atg7*$^{F/F}$ mice (n=3). **D-E:** Liver weight and body weight ratio (%), serum levels of ALT, AST, ALP, and TBA in *Atg7*$^{F/F}$ and *Atg7*$^{\Delta hep}$ mice following alcohol or pair-fed treatment. **F:** Hepatic TG and TCHO levels in *Atg7*$^{F/F}$ and *Atg7*$^{\Delta hep}$ mice given alcohol or pair-fed treatment. Mice were used at the age of 8 to 15 wk, n=3 to 5. **P* < 0.05 versus non-treated F/F control; †*P* < 0.05 versus non-treated ΔHep control, ‡*P* < 0.05 versus treated F/F control.

Fig.4 Constitutive deletion of hepatic *Atg5* does not enhance liver injury in a chronic-plus-binge model. A: Scheme of the chronic-plus-binge alcohol treatment. *Atg7*$^{F/F}$ and *Atg7*$^{\Delta hep\text{-}ERT2}$ mice were injected with TMX at day 3 and day 4 during acclimatization. After

acclimatization, mice were randomly divided into two groups and given a liquid diet with alcohol (EtOH-fed) or with maltose dextrin (Pair-fed) for 10 days, followed by a single gavage of alcohol (5g/kg) or iso-caloric maltose dextrin. Mice were analyzed nine hours later. **B:** Representative western blot images of protein expression in the liver from *Atg5*$^{F/F}$ and *Atg5*$^{\Delta hep}$ mice following alcohol or pair-fed treatment. Anti-ATG12 antibody was used to detect the ATG12-ATG5 conjugate. **C:** The density of ATG5-ATG12, P62, or NQO1 was normalized to that of β-Actin. The density of LC3II was normalized to that of LC3I. These values were expressed as fold change over pair-fed *Atg5*$^{F/F}$ mice (n=4). **D:** The mRNA level of *Gstm1* and *Nqo1* in livers of *Atg5*$^{F/F}$ and *Atg5*$^{\Delta hep}$ mice following alcohol or pair-fed treatment. Expression levels were normalized to that of β-Actin and expressed as the fold change over those of pair-fed *Atg5*$^{F/F}$ (n=6). **E-H:** Liver weight and body weight ratio (%), serum levels of ALT, AST, and ALP in *Atg5*$^{F/F}$ and *Atg5*$^{\Delta hep}$ mice following alcohol or pair-fed treatment (n=7-18). **I-L:**. Hepatic TG and TCHO levels in *Atg5*$^{F/F}$ and *Atg5*$^{\Delta hep}$ mice given alcohol or pair-fed treatment. **P* < 0.05 versus non-treated F/F control; †*P* < 0.05 versus non-treated ΔHep control, ‡*P* < 0.05 versus treated F/F control.

Fig.5 Reduced inflammation and fibrosis in constitutive *Atg5*-deficient livers following chronic-plus-binge alcohol treatment. A-E: *Atg7*$^{F/F}$ and *Atg7*$^{\Delta hep\text{-}ERT2}$ mice (18 to 24 weeks old) were injected with TMX at day 3 and day 4 during acclimatization. After acclimatization, mice were randomly divided into two groups and given a liquid diet with alcohol (EtOH-fed) or with maltose dextrin (Pair-fed) for 10 days, followed by a single gavage of alcohol (5g/kg) or iso-caloric maltose dextrin. Mice were analyzed nine hours later. Liver sections were subjected to hematoxylin and eosin (H-E) staining (**A**), F4/80 stain and quantified (**B-C**), and Masson's trichrome stain and quantified (**D-E**). **F:** The hepatic hydroxyproline level was determined (n=5 to 6). **G:** Representative western blot images of α-SMA protein and densitometric analysis. The density of α-SMA protein was normalized to that of β-Actin and expressed as the fold change

over those of *Atg5*$^{F/F}$ mice given the pair-fed diet (n=4). **H:** The mRNA expression of fibrosis-related genes in the livers of *Atg5*$^{F/F}$ and *Atg5*$^{\Delta hep}$ mice given alcohol or control diet. Expression levels of indicated genes were determined by RT-qPCR and were normalized to that of β-Actin and expressed as the fold change over *Atg5*$^{F/F}$ mice given pair-fed treatment (n=6). **P* < 0.05 versus non-treated F/F control; †*P* < 0.05 versus non-treated ΔHep control, ‡*P* < 0.05 versus treated F/F control. α-SMA: α-smooth muscle actin, *Ctgf*: connective tissue growth factor, Tgf-β: transforming growth factor beta 1, *Timp1*: TIMP metallopeptidase inhibitor 1, and *Gfap*: glial fibrillary acidic protein.

Fig.6 Reduced cholestasis in constitutive *Atg5*-deficient livers following chronic-plus-binge alcohol treatment. A-B: *Atg7*$^{F/F}$ and *Atg7*$^{\Delta hep\text{-}ERT2}$ mice (18 to 24 weeks old) were injected with TMX at day 3 and day 4 during acclimatization. After acclimatization, mice were randomly divided into two groups and given a liquid diet with alcohol (EtOH-fed) or with maltose dextrin (Pair-fed) for 10 days, followed by a single gavage of alcohol (5g/kg) or iso-caloric maltose dextrin. Mice were analyzed nine hours later. Liver sections were immunostained with anti-CK19 (**A**). CK19 positive areas (n=4 to 5) were quantified. **C:** Serum levels of total bile acids (TBA; both sexes, n=11 to 18; Male, n=6 to 12; Female, n=4 to 7). **D-E:** The levels of TBA in each gram of liver (**D**) or in the whole liver (**E**) were determined (all sexes, n=6; male only, n=3; or female only, n=3). **P* < 0.05 versus non-treated F/F control; †*P* < 0.05 versus non-treated ΔHep control, ‡*P* < 0.05 versus treated F/F control. Scale bar: 0.1mm

Fig.7 Constitutive deletion of hepatic *Atg5* alters the expression of genes related to alcohol metabolism and serum alcohol clearance. A-B: *Atg7*$^{F/F}$ and *Atg7*$^{\Delta hep\text{-}ERT2}$ mice (18 to 24 weeks old) were injected with TMX at day 3 and day 4 during acclimatization. After acclimatization, mice were randomly divided into two groups and given a liquid diet with alcohol (EtOH-fed) or with maltose dextrin (Pair-fed) for 10 days, followed by a single gavage of alcohol (5g/kg) or iso-caloric maltose dextrin. Mice were analyzed nine hours later. The mRNA levels of

genes related to the oxidation of alcohol (**A**) or acetaldehyde (**B**) in the liver (n=6). **C:** The protein levels of key alcohol metabolizing enzymes in the liver. β-Actin (for Cyp2E1) and GAPDH (for ALDH1/2 and ADH) were used as loading control. **D:** Densitometry was conducted, and the density levels were normalized to that of loading control and expressed as fold change over *Atg5*$^{F/F}$ mice given pair-fed treatment (n=4). **E:** *Atg5*$^{F/F}$ and *Atg5*$^{\Delta hep}$ mice at the age of 13 to 20 wk were given a single dose of alcohol binge (5 g/kg, n=3 to 5). Plasma alcohol concentration were then measured at 1, 3, and 9 hours later. **P* < 0.05 versus non-treated F/F control; †*P* < 0.05 versus non-treated ΔHep control, ‡*P* < 0.05 versus treated F/F control (**A, B**, and **D**); ****P* < 0.001 (**E**).

Table 1. Antibody list.

Antibody name	Company	Catalog #	Host
ACTIN (8H10D10))	Cell Signaling	3700	mouse
ADH	Santa Cruz	sc-133207	mouse
ALDH1/2	Santa Cruz	sc-166362	mouse
ATG12	Cell Signaling	2011	rabbit
ATG7	Cell Signaling	2631	rabbit
CK19	DSHB	TROMA-III	Rat
CYP2E1	Enzo Life Sciences	BML-CR3271	Rabbit
GAPDH	Novus biologicals	NB 300-221	mouse
LC3B	Sigma	L7543	rabbit
NQO1	Abcam	ab34173	rabbit
SQSTM1/P62	Abnova	H00008878-M01	mouse
Smooth Muscle Actin (α-SMA)	Thermo	PA5-19465	rabbit

Table 2. Primer list.

Gene/primer name	Sequence (Forward)	Sequence (Reverse)
Acaca	5'-GCCTCTTCCTGACAAACGAG-3'	5'-TGACTGCCGAAACATCTCTG-3'
Acadl	5'-GGTGGAAAACGGAATGAAAGG-3'	5'-GGCAATCGGACATCTTCAAAG-3'
Acadm	5'-TGTTAATCGGTGAAGGAGCAG-3'	5'-CTATCCAGGGCATACTTCGTG-3'
Acox1	5'-CATATGACCCCAAGACCCAAG-3'	5'-CATGTAACCCGTAGCACTCC-3'
Actin	5'-ACTATTGGCAACGAGCGGTT-3'	5'-CAGGATTCCATACCCAAGAAGGA-3'
Adh1	5'-TGTTGAGAGCGTTGGAGAAG-3'	5'-CGCTTCGGCTACAAAAGTTG-3'
Adh4	5'-GTAGACTCTGTCCCAAACCTG-3'	5'-AAGGTCAGGATTGTTCGGATG-3'
Adh5	5'-AAATCTCCACTCGTCCATTCC-3'	5'-CACTCTCCACACTCTTCCATC-3'
Adh7	5'-GGTTGTGGAGAGTGTTGGAG-3'	5'-CCTGTCAGATCGCTCCTAATG-3'
Akr1d1	5'-CTCATTGGGCTTGGAACCTA-3'	5'-CATTGATGGGACATGCTCTG-3'
Aldh16a1	5'-GAGGTTCGAGATGGAGATGTG-3'	5'-AAAGAGAAAGGAGTCGGCAG-3'
Aldh18a1	5'-CAGACATCGTGGAGGGAAAG-3'	5'-CTGTTCAGGCTCTAAGGTAGC-3'
Aldh1a1	5'-ATCACTGTGTCATCTGCTCTG-3'	5'-CCCAGTTCTCTTCCATTTCCAG-3'
Aldh1a2	5'-ATGGATGCGTCTGAAAGAGG-3'	5'-TGACTCCCTGCAAATCGATG-3'
Aldh1a3	5'-AACAAGATAGCCTTCACCGG-3'	5'-CCAAGTCCAAGTCAGCATCT-3'
Aldh1b1	5'-GGAGTCTTATGTCTTGGATCTGG-3'	5'-TGTCGGGTGAAGCAGAAATG-3'
Aldh1l1	5'-CATCCAGACCTTCCGATACTTC-3'	5'-ACAATACCACAGACCCCAAC-3'
Aldh1l2	5'-CATTGACAGCCCAAAGCATG-3'	5'-CCCAGAAAACAGAAAACCCAG-3'
Aldh2	5'-TGCAGGAGAATGTGTATGACG-3'	5'-CGATTTGATGTAGCCGAGGATC-3'
Aldh3a1	5'-GGCGTGGTCCTTGTCATAG-3'	5'-AGGGATAAGTGTTGAAAGCAGG-3'
Aldh3a2	5'-AGCCCTTGTTACATTGACAGAG-3'	5'-TTCATGTACTTTCCCCAGGC-3'
Aldh3b1	5'-CCTTCGGTCTGGTGCTTATC-3'	5'-ACCTCAGCCAGTATCTTTTCAG-3'
Aldh3b2	5'-GAATCAGATGTTGGAACGCAC-3'	5'-GGAGAAGGTGTCAAAGGAGAAC-3'
Aldh4a1	5'-CGATAAGTCTACTGGGTCTGTG-3'	5'-GGGCTTATGAGTCTCCTTGATG-3'
Aldh5a1	5'-CCAAGATCATAACAGCCGAGAG-3'	5'-TCGCTTATCTTTGGCAGAGG-3'
Aldh6a1	5'-AAGGGAAGACTCTTGCTGATG-3'	5'-GAGGCAGACGGTAGGAATAAAG-3'

Aldh7a1	5’-AGATATTCCTGCCCCAAAACG-3’	5’-CTGAACCTCGCCTATTCCTTC-3’
Aldh8a1	5’-GTATGCATTACACCGTTCGC-3’	5’-AAGTCATCTCACTGGGCTTG-3’
Aldh9a1	5’-CTGGAATACTATGCAGGGCTG-3’	5’-GCGATCTGGAAGGGATAGTTC-3’
Apob	5’-ATTCGAGCACAGATGACCAG-3’	5’-GTACCTTTCACCATCAGACTCC-3’
Apoe	5’-CAATTGCGAAGATGAAGGCTC-3’	5’-TAATCCCAGAAGCGGTTCAG-3’
Bsep	5’-CTGCCAAGGATGCTAATGCA-3’	5’-CGATGGCTACCCTTTGCTTCT-3’
Cat	5’-CTCGTTCAGGATGTGGTTTTC-3’	5’-CTTTCCCTTGGAGTATCTGGTG-3’
Ccl2	5’-GTCCCTGTCATGCTTCTGG-3’	5’-GCTCTCCAGCCTACTCATTG-3’
Ccl3	5’-TTCTCTGTACCATGACACTCTGC-3’	5’-CGTGGAATCTTCCGGCTGTAG-3’
Ccr2	5’-GCTCTACATTCACTCCTTCCAC-3’	5’-ACCACTGTCTTTGAGGCTTG-3’
Cd36	5’-GCGACATGATTAATGGCACAG-3’	5’-GATCCGAACACAGCGTAGATAG-3’
Collagen-1l	5’-ACGGCTGCACGAGTCACAC-3’	5’-GGCAGGCGGGAGGTCTT-3’
Ctgf	5’-GGGCCTCTTCTGCGATTTC-3’	5’-ATCCAGGCAAGTGCATTGGTA-3’
Cyp27a1	5’-GCCTCACCTATGGGATCTTCA-3’	5’-TCAAAGCCTGACGCAGATG-3’
Cyp2e1	5’-TCACTGGACATCAACTGCC-3’	5’-TGGTCTCTGTTCCTGCAAAG-3’
Cyp3A11	5’-CAGAAGCACCGAGTGGATTT-3’	5’-GACTGGGCTGTGATCTCCAT-3’
Cyp7a1	5’-AACAACCTGCCAGTACTAGATAGC-3’	5’-GTGTAGAGTGAAGTCCTCCTTAGC-3’
Cyp7b1	5’-CAGCTATGTTCTGGGCAATG-3’	5’-TCGGATGATGCTGGAGTATG-3’
Cyp8b1	5’-AGTACACATGGACCCCGACATC-3’	5’-GGGTGCCATCCGGGTTGAG-3’
F4/80	5’-TGCATCTAGCAATGGACAGC-3’	5’-GCCTTCTGGATCCATTTGAA-3’
Fabp1	5’-TCTCCGGCAAGTACCAATTG-3’	5’-TTGATGTCCTTCCCTTTCTGG-3’
Fasn	5’-CCCTTGATGAAGAGGGATCA-3’	5’-ACTCCACAGGTGGGAACAAG-3’
Fgfr4	5’-CTGCCAGAGGAAGACCTCAC-3’	5’-GTAGTGGCCACGGATGACTT-3’
Fxr *(Nr1h4)*	5’-GGCCTCTGGGTACCACTACA-3’	5’-TGTACACGGCGTTCTTGGTA-3’
Gfap	5’-GAAAACCGCATCACCATTCC-3’	5’-CTTAATGACCTCACCATCCCG-3’
Gstm1	5’-ACTTGATTGATGGGGCTCAC-3’	5’-TCTCCAAAATGTCCACACGA-3’
Hsd3b7	5’-CCATCCACAAAGTCAACGTG-3’	5’-CTCCATTGACCTTCCTTCCA-3’
Ifng	5’-GATGCATTCATGAGTATTGCCAAGT-3’	5’-GTGGACCACTCGGATGAGCTC-3’
Il6	5’-AGTTGCCTTCTTGGGACTGA-3’	5’-TCCACGATTTCCCAGAGAAC-3’

Lcn2	5'-CTACAATGTCACCTCCATCCTG-3'	5'-ACCTGTGCATATTTCCCAGAG-3'
Lipe (*Hsl*)	5'-CTGAGATTGAGGTGCTGTCG-3'	5'-CAAGGGAGGTGAGATGGTAAC-3'
Lpl	5'-AACAAGGTCAGAGCCAAGAG-3'	5'-CCATCCTCAGTCCCAGAAAAG-3'
Ly6g	5'-CACCTGAGACTTCCTGCAAC-3'	5'-CTTCTATCTCCAGAGCAACGC-3'
Mrp2 *(Abcc2)*	5'-GCACTGTAGGCTCTGGGAAG-3'	5'-TGCTGAGGGACGTAGGCTAT-3'
Mrp3	5'-GGACTTCCAGTGCTCAGAGG-3'	5'-AGCTGTGGCCTCGTCTAAAA-3'
Mrp4	5'-TGTTTGATGCACACCAGGAT-3'	5'-GACAAACATGGCACAGATGG-3'
Nqo1	5'-GCACTGATCGTACTGGCTCA-3'	5'-CATGGCATAGAGGTCCGACT-3'
Ost-α	5'-GTCTCAAGTGATGAACTGCCA-3'	5'-TTGAGTGCTGAGTCCAGGTC-3'
Ost-β	5'-GTATTTTCGTGCAGAAGATGCG-3'	5'-TTTCTGTTTGCCAGGATGCTC-3'
Pnpla2 (*Atgl*)	5'-ATATCCCACTTTAGCTCCAAGG-3'	5'-CAAGTTGTCTGAAATGCCGC-3'
Pparg	5'-ATGCCAGTACTGCCGTTTTC-3'	5'-GGCCTTGACCTTGTTCATGT-3'
Saa2	5'-CAGGATGAAGCTACTCACCAG-3'	5'-CTTCATGTCAGTGTAGGCTCG-3'
Scd1	5'-TTCTTACACGACCACCACCA-3'	5'-CCGAAGAGGCAGGTGTAGAG-3'
Slc10a1* (Ntcp*)	5'-CACCATGGAGTTCAGCAAGA-3'	5'-CCAGAAGGAAAGCACTGAGG-3'
Slco1a1 *(Oatp1)*	5'-ATCCAGTGTGTGGGGACAAT-3'	5'-GCAGCTGCAATTTTGAAACA-3'
Tgfb	5'-CACCGGAGAGCCCTGGATA-3'	5'-TGTACAGCTGCCGCACACA-3'
Timp1	5'-ATTCAAGGCTGTGGGAAATG-3'	5'-CTCAGAGTACGCCAGGGAAC-3'
Tlr4	5'-TTCAGAACTTCAGTGGCTGG-3'	5'-TGTTAGTCCAGAGAAACTTCCTG-3'

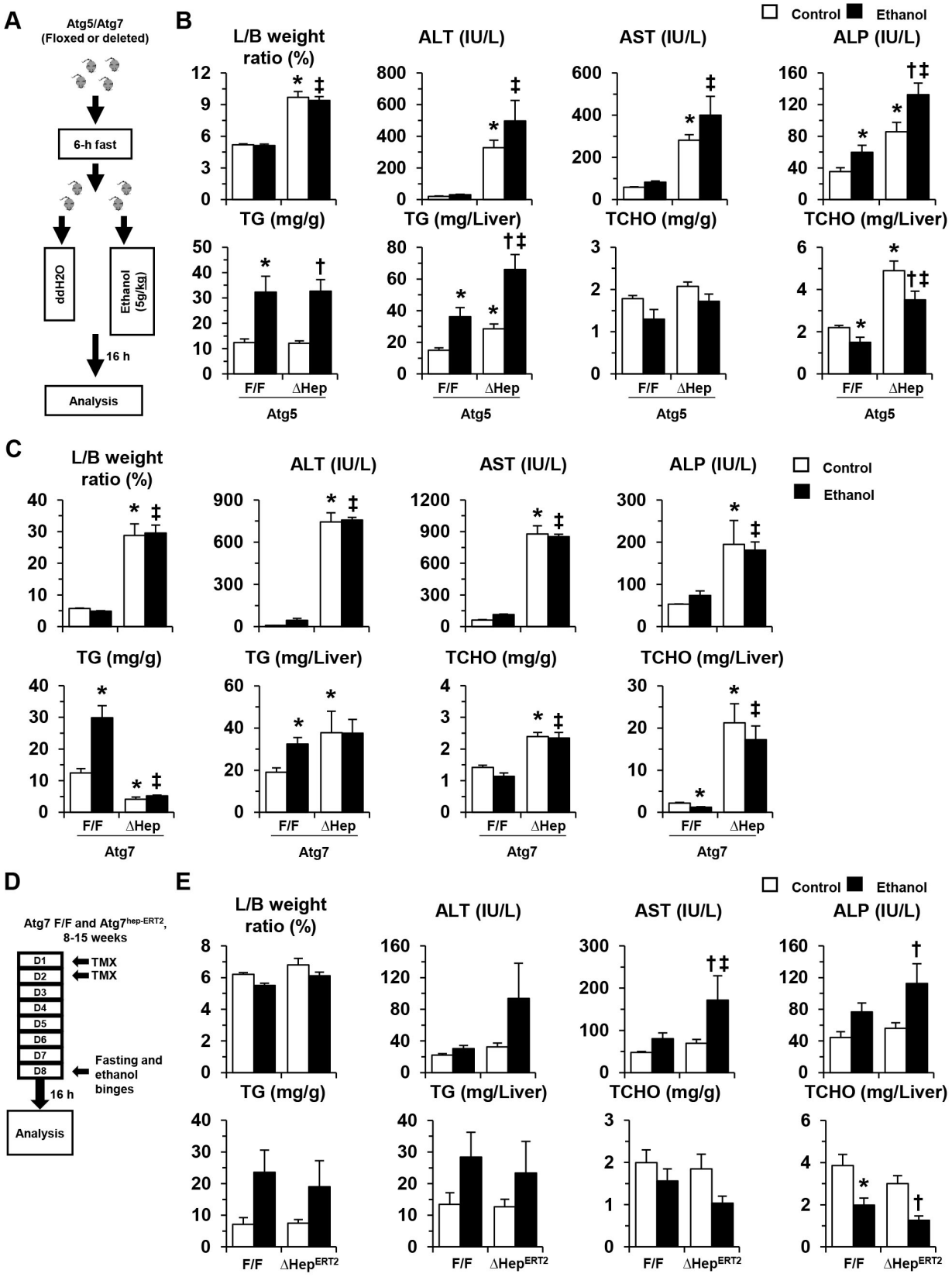
A
Atg5/Atg7
(Floxed or deleted)
6-h fast
ddH2O
Ethanol
(5g/kg)
16 h
Analysis
B
Control
Ethanol
L/B weight ratio (%)
ALT (IU/L)
AST (IU/L)
ALP (IU/L)
TG (mg/g)
TG (mg/Liver)
TCHO (mg/g)
TCHO (mg/Liver)
F/F
ΔHep
Atg5
C
L/B weight ratio (%)
ALT (IU/L)
AST (IU/L)
ALP (IU/L)
TG (mg/g)
TG (mg/Liver)
TCHO (mg/g)
TCHO (mg/Liver)
Control
Ethanol
F/F
ΔHep
Atg7
D
Atg7 F/F and Atg7hep-ERT2,
8-15 weeks
D1
D2
D3
D4
D5
D6
D7
D8
TMX
TMX
Fasting and
ethanol
binges
16 h
Analysis
E
Control
Ethanol
L/B weight ratio (%)
ALT (IU/L)
AST (IU/L)
ALP (IU/L)
TG (mg/g)
TG (mg/Liver)
TCHO (mg/g)
TCHO (mg/Liver)
F/F
ΔHepERT2

Fig. 2

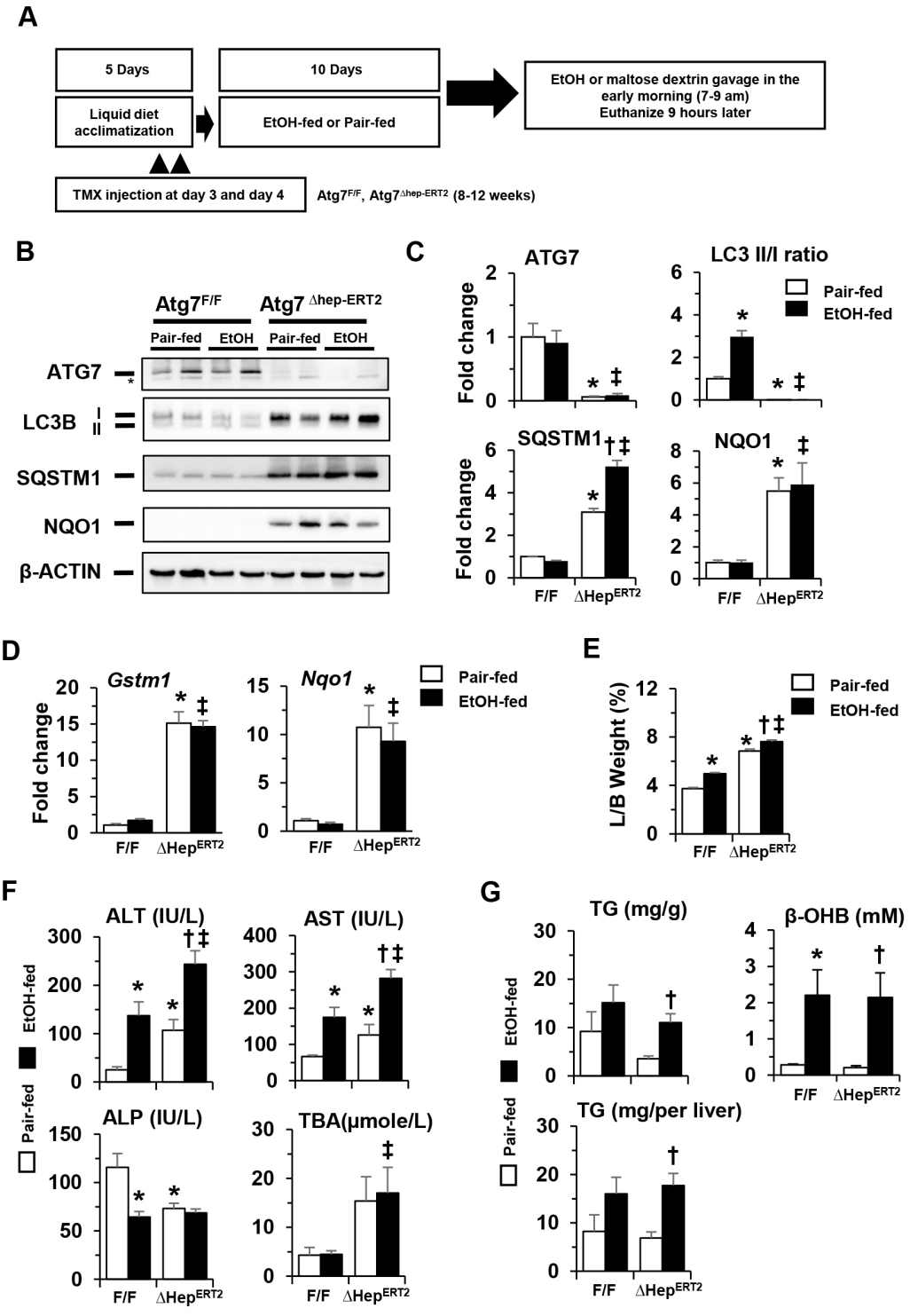
A
5 Days
Liquid diet acclimatization
10 Days
EtOH-fed or Pair-fed
EtOH or maltose dextrin gavage in the early morning (7-9 am)
Euthanize 9 hours later
TMX injection at day 3 and day 4
Atg7F/F, Atg7Δhep-ERT2 (8-12 weeks)
B
Atg7F/F
Atg7 Δhep-ERT2
Pair-fed
EtOH
Pair-fed
EtOH
ATG7
LC3B I II
SQSTM1
NQO1
β-ACTIN
C
ATG7
LC3 II/I ratio
Pair-fed
EtOH-fed
Fold change
SQSTM1
NQO1
F/F
ΔHepERT2
D
Gstm1
Nqo1
Pair-fed
EtOH-fed
Fold change
F/F
ΔHepERT2
E
L/B Weight (%)
Pair-fed
EtOH-fed
F/F
ΔHepERT2
F
ALT (IU/L)
AST (IU/L)
ALP (IU/L)
TBA(μmole/L)
EtOH-fed
Pair-fed
F/F
ΔHepERT2
G
TG (mg/g)
β-OHB (mM)
TG (mg/per liver)
EtOH-fed
Pair-fed
F/F
ΔHepERT2

Fig. 3

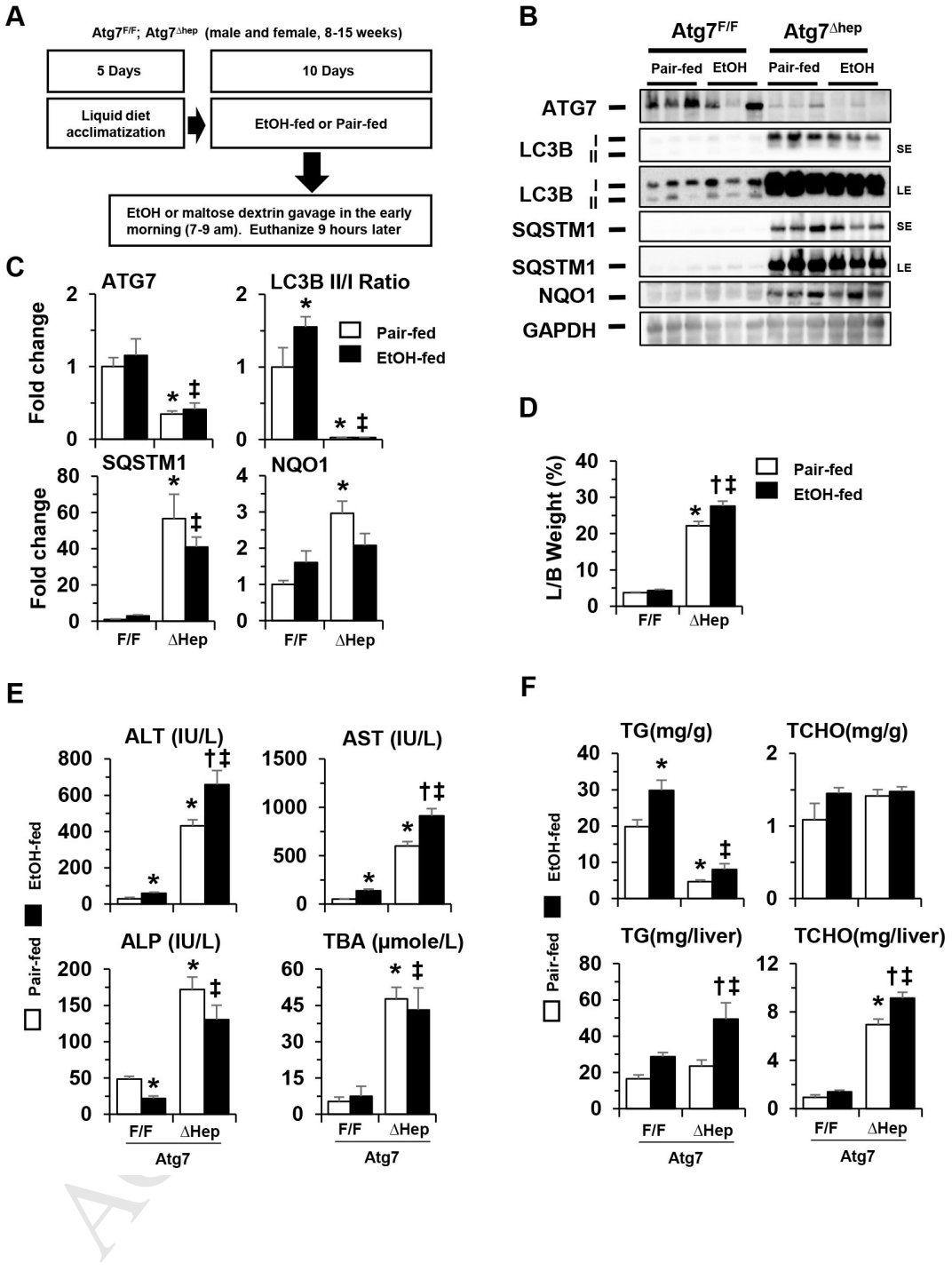
A
Atg7F/F; Atg7Δhep (male and female, 8-15 weeks)
5 Days
10 Days
Liquid diet acclimatization
EtOH-fed or Pair-fed
EtOH or maltose dextrin gavage in the early morning (7-9 am). Euthanize 9 hours later
B
Atg7F/F
Atg7Δhep
Pair-fed
EtOH
Pair-fed
EtOH
ATG7
LC3B II
LC3B I
SE
LC3B II
LC3B I
LE
SQSTM1
SE
SQSTM1
LE
NQO1
GAPDH
C
ATG7
LC3B II/I Ratio
Pair-fed
EtOH-fed
Fold change
SQSTM1
NQO1
Fold change
F/F
ΔHep
F/F
ΔHep
D
L/B Weight (%)
Pair-fed
EtOH-fed
F/F
ΔHep
E
ALT (IU/L)
AST (IU/L)
EtOH-fed
Pair-fed
ALP (IU/L)
TBA (μmole/L)
F/F
ΔHep
Atg7
F/F
ΔHep
Atg7
F
TG(mg/g)
TCHO(mg/g)
EtOH-fed
Pair-fed
TG(mg/liver)
TCHO(mg/liver)
F/F
ΔHep
Atg7
F/F
ΔHep
Atg7

Fig. 4

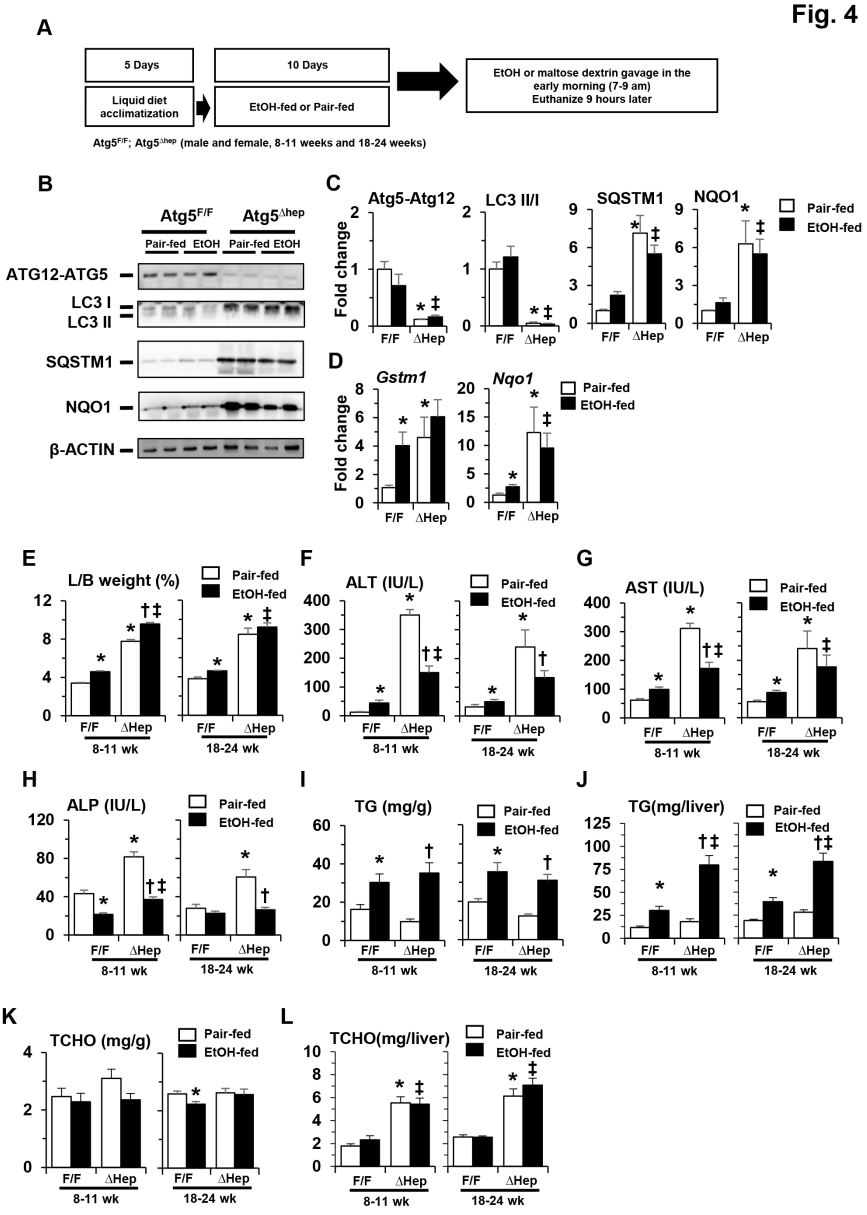
A
5 Days
Liquid diet acclimatization
10 Days
EtOH-fed or Pair-fed
EtOH or maltose dextrin gavage in the early morning (7-9 am)
Euthanize 9 hours later
Atg5F/F; Atg5ΔHep (male and female, 8-11 weeks and 18-24 weeks)
B
Atg5F/F
Atg5ΔHep
Pair-fed EtOH Pair-fed EtOH
ATG12-ATG5
LC3 I
LC3 II
SQSTM1
NQO1
β-ACTIN
C
Atg5-Atg12
LC3 II/I
SQSTM1
NQO1
Fold change
Pair-fed
EtOH-fed
F/F
ΔHep
D
Gstm1
Nqo1
E
L/B weight (%)
F
ALT (IU/L)
G
AST (IU/L)
H
ALP (IU/L)
I
TG (mg/g)
J
TG(mg/liver)
K
TCHO (mg/g)
L
TCHO(mg/liver)
8-11 wk
18-24 wk

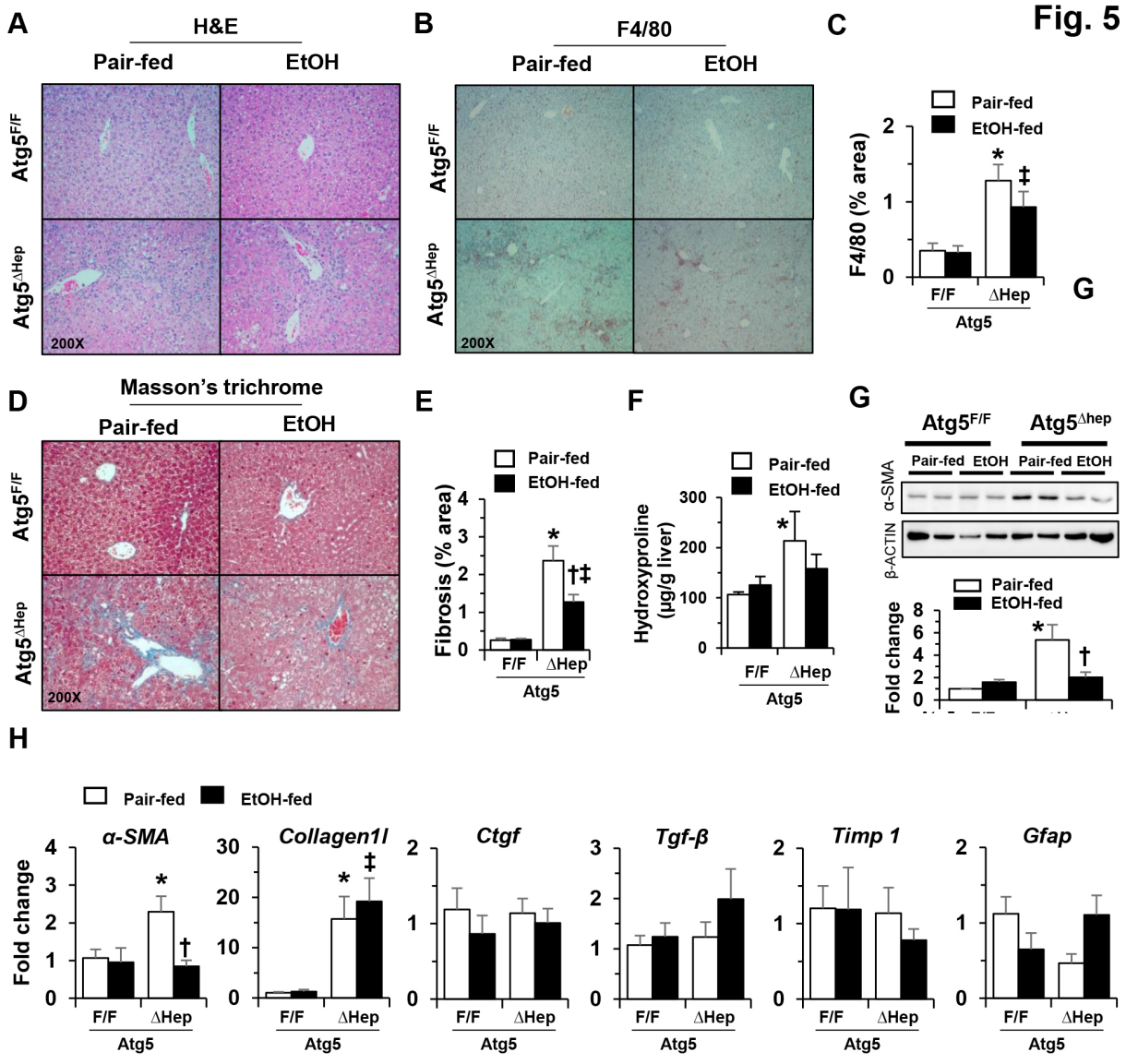

Fig. 5

Fig. 6

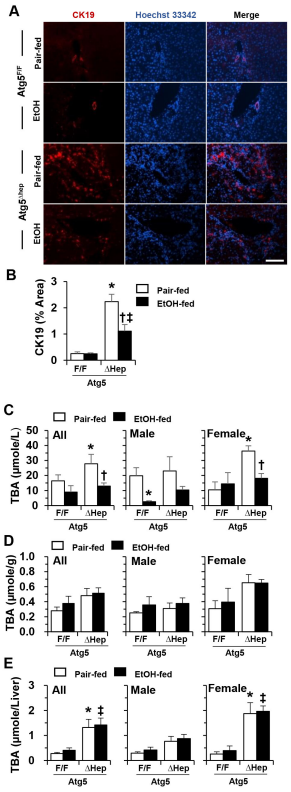

Fig. 7